Molecular Pharmacology Fast Forward. Published on May 29, 2009 as DOI: 10.1124/mol.109.056309
This article has not been copyedited and formatted. The final version may differ from this version.

BCL-2 family inhibitors enhance HDACI+sorafenib lethality via autophagy and overcome blockade of the extrinsic pathway to facilitate killing.

Aditi Pandya Martin[*], Margaret A. Park[*], Clint Mitchell[*], Teneille Walker, Mohamed Rahmani,

Andrew Thorburn, Dieter Häussinger, Roland Reinehr, Steven Grant, and Paul Dent[#]

Departments of Biochemistry (APM, MAP, CM, TW, SG, PD), Medicine (MR, SG), Institute for Molecular Medicine (SG, PD), Virginia Commonwealth University, 401 College St., Richmond, VA 23298; Clinic for Gastroenterology (DH, RR), Hepatology and Infectiology, Heinrich-Heine-University Düsseldorf, Düsseldorf, Germany; Department of Pharmacology (AT), School of Medicine, University of Colorado Denver, Aurora, CO 80045, USA.

Molecular Pharmacology Fast Forward. Published on May 29, 2009 as DOI: 10.1124/mol.109.056309
This article has not been copyedited and formatted. The final version may differ from this version.

Running Title: HDACIs, Obatoclax and Sorafenib.

Abbreviations: Vor.: Vorinostat; Sor.: Sorafenib; Val.: sodium valproate; ERK: extracellular regulated kinase; MEK: mitogen activated extracellular regulated kinase; EGF: epidermal growth factor; PARP: poly ADP ribosyl polymerase; PI3K: phosphatidyl inositol 3 kinase; -/-: null / gene deleted; ERK: extracellular regulated kinase; MAPK: mitogen activated protein kinase; MEK: mitogen activated extracellular regulated kinase; R: receptor; JNK: c-Jun NH_2-terminal kinase; dn: dominant negative; P: phospho-; ca: constitutively active; WT: wild type.

#Correspondence to:
Paul Dent, Ph.D.
Department of Biochemistry and Molecular Biology
401 College Street, Massey Cancer Center,
Room 280a, Box 980035
Virginia Commonwealth University
Richmond VA 23298-0035.
Tel: 804 628 0861
Fax: 804 827 1309
pdent@vcu.edu

Number of text pages: 39
Number of Tables: 3
Number of Figures: 7
Words in Abstract: 248
Words in Introduction: 809
Words in Discussion: 1,454

Molecular Pharmacology Fast Forward. Published on May 29, 2009 as DOI: 10.1124/mol.109.056309
This article has not been copyedited and formatted. The final version may differ from this version.

Abstract.

We examined whether the multi-kinase inhibitor sorafenib and histone deacetylase inhibitors (HDACI) interact to kill pancreatic carcinoma cells, and determined the impact of inhibiting BCL-2 family function on sorafenib and HDACI lethality. The lethality of sorafenib was enhanced in pancreatic tumor cells in a synergistic fashion by pharmacologically achievable concentrations of the HDACIs vorinostat or sodium valproate. Over-expression of c-FLIP-s or knock down of CD95 suppressed sorafenib + HDACI lethality. In immunohistochemical analyses or using expression of fluorescent tagged proteins, sorafenib+vorinostat treatment promoted co-localization of CD95 with caspase 8; and CD95 association with the ER markers calnexin, ATG5 and Grp78/BiP. In cells lacking CD95 expression or in cells expressing c-FLIP-s the lethality of sorafenib + HDACI exposure was abolished, which was restored when cells were co-exposed to BCL-2 family inhibitors (HA14-1, GX15-070). Knock down of BCL-2, BCL-XL and MCL-1 recapitulated the effects of GX15-070 treatment. Knock down of BAX and BAK modestly reduced sorafenib + HDACI lethality but abolished the effects of GX15-070 treatment. Sorafenib + HDACI exposure generated a CD95- and Beclin1-dependent protective form of autophagy whereas GX15-070 treatment generated a Beclin1-dependent toxic form of autophagy. The potentiation of sorafenib + HDACI killing by GX15-070 was suppressed by knock down of Beclin1 or of BAX+BAK. Our data demonstrate that pancreatic tumor cells are susceptible to sorafenib + HDACI lethality and that in tumor cells unable to signal death from CD95, use of a BCL-2 family antagonist facilitates sorafenib + HDACI killing via autophagy and the intrinsic pathway.

Molecular Pharmacology Fast Forward. Published on May 29, 2009 as DOI: 10.1124/mol.109.056309
This article has not been copyedited and formatted. The final version may differ from this version.

Introduction.

In the United States, pancreatic carcinomas have 5 year survival rates of less than 5% (Parkin et al, 2005; Bardeesy and De Pinho, 2002). These statistics emphasize the need to develop original therapies using novel targeted agents against this lethal malignancy.

Tumor cells utilize a wide variety of mechanisms to maintain cell viability, including loss of death receptor expression, e.g. CD95, by reducing expression of pro-apoptotic BH3 domain proteins, e.g. BAX, or by increasing expression of anti-apoptotic BCL-2 family members, e.g. MCL-1 (Kang and Reynolds, 2009; Susnow et al, 2009; Lessene et al, 2008). In the case of protective BCL-2 family proteins, several clinically relevant small molecule inhibitors have been developed that specifically bind to the BCL-2 family protein, without altering expression of the protein, and block the binding of pro-apoptotic BH3 domain proteins, e.g. ABT-737; GX15-070 (Azmi and Mohammad, 2009; Zhang et al., 2007). The dissociation of protective BCL-2 proteins from toxic BH3 domain proteins results in greater levels of free BH3 domain protein that will facilitate mitochondrial dysfunction, promote pore formation with alterations in mitochondrial permeability, and facilitate the lethality of other therapeutic agents (Dai and Grant, 2007; Chen et al, 2007).

The apoptotic threshold in tumor cells is also controlled by the activities of multiple signal transduction pathways. The Raf-MEK1/2-ERK1/2 pathway is frequently dysregulated in neoplastic transformation and, along with the MEK5-ERK5, c-Jun NH_2-terminal kinase (JNK1/2) and p38 MAPK pathways, is a member of the MAPK super-family (Dent et al., 2009; Dent et al, 2005; Dent et al., 2003; Valerie et al, 2007). These protein kinases are involved in responses to diverse mitogens and environmental stresses and have also been implicated in cell survival processes, with activation of the ERK1/2 pathway being associated with survival, and JNK1/2 and p38 MAPK pathway signaling with apoptosis. A number of anti-apoptotic effector proteins have been identified downstream of ERK1/2 signaling, including increased expression of anti-apoptotic proteins such as c-FLIP-s, as well as protective BCL-2 family proteins such as BCL-XL and MCL-1 (Grant and Dent, 2004;

Molecular Pharmacology Fast Forward. Published on May 29, 2009 as DOI: 10.1124/mol.109.056309
This article has not been copyedited and formatted. The final version may differ from this version.

Allan et al, 2003; Mori et al, 2003; Ley et al, 2003; Wang et al, 2007; Qiao et al, 2003). In view of the importance of the ERK1/2 pathway in tumor cell growth and survival, inhibitors have been developed that have entered clinical trials, including sorafenib (Bay 43-9006, Nexavar®; a Raf kinase inhibitor) and AZD6244 (a MEK1/2 inhibitor) (Li et al, 2007; Davies et al., 2007).

Sorafenib is a multi-kinase inhibitor that was originally developed as an inhibitor of Raf-1, but which was subsequently shown to inhibit multiple other kinases, including class III tyrosine kinase receptors such as platelet-derived growth factor, vascular endothelial growth factor receptors 1 and 2, c-Kit and FLT3 (Flaherty, 2007). Some of the anti-tumor effects of sorafenib have been ascribed to anti-angiogenic actions of this agent through inhibition of the growth factor receptors (Rini, 2006; Strumberg, 2005; Gollob, 2005). Several groups have shown *in vitro* that sorafenib kills human leukemia cells at concentrations below the maximum achievable dose (C_{max}) of 15-20 μM, through a mechanism involving down-regulation of the anti-apoptotic BCL-2 family member MCL-1 (Rahmani et al, 2005; Rahmani et al, 2007a). In these studies sorafenib-mediated MCL-1 down-regulation occurred through a translational rather than a transcriptional or post-translational process that was mediated by endoplasmic reticulum (ER) stress signaling through PKR-like endoplasmic reticulum kinase (PERK) (Rahmani et al, 2007b; Dasmahapatra et al, 2007).

Histone deacetylase inhibitors (HDACI) represent a class of agents that act by blocking histone de-acetylation, thereby modifying chromatin structure and gene transcription. HDACs, along with histone acetyl-transferases, reciprocally regulate the acetylation status of the positively charged NH_2-terminal histone tails of nucleosomes. HDACIs promote histone acetylation and neutralization of positively charged lysine residues on histone tails, allowing chromatin to assume a more open conformation, which favors transcription (Gregory et al, 2001). However, HDACIs also induce acetylation of other non-histone targets, actions that may have plieotropic biological consequences, including inhibition of HSP90 function, induction of oxidative injury and in some systems up-regulation of death receptor expression (Marks et al, 2003; Bali et al, 2005; Kwon et al, 2002). With respect to combinatorial drug studies with a multi-kinase inhibitor such as sorafenib, HDACIs are of interest in

Molecular Pharmacology Fast Forward. Published on May 29, 2009 as DOI: 10.1124/mol.109.056309
This article has not been copyedited and formatted. The final version may differ from this version.

that they have potential to down-regulate multiple oncogenic kinases by interfering with HSP90 function, leading to proteasomal degradation of these proteins.

We recently demonstrated that sorafenib synergized with vorinostat to kill liver and kidney cancer cells in a CD95-dependent fashion (Zhang et al., 2008; Park et al, 2008a). Our data also suggested that proteins involved in ER stress signaling co-immunoprecipitated with activated CD95 in hepatoma cells and played a regulatory role in cell survival. The present studies determined whether similar mechanisms of drug action apply in pancreatic tumor cells and whether in liver and pancreatic tumor cells restriction or lack of death receptor signaling which blocks sorafenib+HDACI -induced lethality can be subverted by use of BCL-2 family antagonists.

Molecular Pharmacology Fast Forward. Published on May 29, 2009 as DOI: 10.1124/mol.109.056309
This article has not been copyedited and formatted. The final version may differ from this version.

Materials and Methods.

Materials. Sorafenib tosylate was generously provided by Bayer Inc. and the National Cancer Institute, NIH. Vorinostat was generously provided by Merck & Co., Inc. and the National Cancer Institute, NIH. GX15-070 was generously provided by Gemin X Pharmaceuticals and the National Cancer Institute, NIH (Bethesda, MD). The BCL-2/BCL-XL inhibitor HA14-1 was purchased from Calbiochem (San Diego, CA). Phospho-/total-(ERK1/2; JNK1/2; p38 MAPK) antibodies, phospho-/total-AKT (T308; S473) and the total and cleaved caspase 3 antibodies were purchased from Cell Signaling Technologies (Worcester, MA). Anti-BID antibodies were purchased from Cell Signaling Technologies (Worcester, MA). All the secondary antibodies were purchased from Santa Cruz Biotechnology (Santa Cruz, CA). TUNEL kits were purchased from NEN Life Science Products (NEN Life Science Products, Boston, MA) and Boehringer Mannheim (Manheim, Germany), respectively. Trypsin-EDTA, DMEM, RPMI, penicillin-streptomycin were purchased from GIBCOBRL (GIBCOBRL Life Technologies, Grand Island, NY). HEPG2, HEP3B, HuH7 (hepatoma); ASPC-3, MiaPaCa2, PANC1 (pancreatic) cells were purchased from the ATCC. BAK -/-, BAK -/-, BAX+BAK -/-, fibroblasts were kindly provided by Dr. S. Korsmeyer (Harvard University, Boston, MA). Commercially available validated short hairpin RNA molecules to knock down RNA / protein levels were from Qiagen (Valencia, CA): CD95 (SI02654463; SI03118255); ATG5 (SI02655310); Beclin 1 (SI00055573, SI00055587); BAX (SI02662401; SI02654533); BAK (SI00299376; SI02654512). We also made use for confirmatory purposes of the short hairpin RNA construct targeting *ATG5* (pLVTHM/Atg5) that was a gift from Dr. Yousefi, Department of Pharmacology, University of Bern, Switzerland. The plasmids to express green fluorescent protein (GFP)-tagged human LC3; wild type and dominant negative PERK (Myc-tagged PERKΔC); yellow florescent protein (YFP)- tagged CD95; and GFP-tagged FADD were kindly provided by Dr. S. Spiegel, VCU, Dr. J.A. Diehl University of Pennsylvania, Philadelphia, PA, Dr. Reinehr and Dr. Thorburn, respectively. Reagents and performance of experimental procedures were described in (Rahmani et al, 2007b; Dasmahapatra et al, 2007; Zhang et al, 2008; Park et al, 2008a; Park et al, 2008b; Park et al, 2008c; Yacoub et al, 2008; Mitchell et al, 2007; Qiao et al, 2001).

Molecular Pharmacology Fast Forward. Published on May 29, 2009 as DOI: 10.1124/mol.109.056309
This article has not been copyedited and formatted. The final version may differ from this version.

Methods.

Culture and in vitro exposure of cells to drugs. All established cell lines (HEPG2, HEP3B, HuH7 (hepatoma); ASPC-3, MiaPaCa2, PANC1 (pancreatic); Wild type, BAK -/-, BAK -/-, BAX+BAK -/-, transformed mouse embryonic fibroblasts) were cultured at 37 ^{o}C (5% (v/v CO_2) *in vitro* using RPMI supplemented with 5% (v/v) fetal calf serum and 10% (v/v) Non-essential amino acids. For short term cell killing assays, immunoblotting and cytochrome c release / BH3 domain protein activation studies, cells were plated at a density of 3 x 10^3 per cm^2 (~2 x 10^5 cells per well of a 12 well plate) and 48h after plating treated with various drugs. Hepatoma cells were treated with 3 μM sorafenib, 500 nM vorinostat or 1 mM sodium valproate, unless otherwise indicated. Pancreatic cancer cells were treated with 6 μM sorafenib, 500 nM vorinostat or 1 mM sodium valproate, unless otherwise indicated. Unless otherwise indicated GX15-070 and HA14-1 treatments were 100 nM and 10 μM, respectively. *In vitro* vorinostat, sorafenib, and GX15-070 treatments were from 100 mM stock solutions of each drug and the maximal concentration of Vehicle (DMSO) in media was 0.02% (v/v). Sodium valproate was from a stock 1M solution. Cells were not cultured in reduced serum media during any study in this manuscript.

In vitro cell treatments, microscopy, SDS-PAGE and Western blot analysis. For in vitro analyses of short-term cell death effects, cells plated in triplicate were treated with Vehicle or vorinostat or Na valproate / sorafenib for the indicated times in the Figure legends. For apoptosis assays where indicated, cells were pre-treated with vehicle (VEH, DMSO) and therapeutic drugs; floating and attached cells were isolated at the indicated times (24-96h), and subjected to trypan blue cell viability assay by counting in a light microscope. Alternatively, the Annexin V/propidium iodide assay was carried to determine cell viability out as per the manufacturer's instructions (BD PharMingen) using a Becton Dickinson FACScan flow cytometer (Mansfield, MA). Vorinostat or Na valproate / sorafenib lethality, as judged by annexin-PI, was first evident ~24h after drug exposure (data not shown). Data are plotted as either percentage cell death or the true percentage of cell death with the amount of cell killing in vehicle treated cells subtracted from the total. For microscopy, cells were plated into 8 chambered glass slides and 24h later treated with drugs. Six h after drug treatment cells were fixed and

permeabilized. Cells were stained with the indicated primary antibodies (CD95; Grp78/BiP; ATG5; CD95; Calnexin) and visualized with secondary antibodies with conjugated fluorescent probes (FITC, PE). Cells were visualized using the appropriate fluorescent light filters at 40X and images merged using Adobe Photoshop CS2. Areas of protein-protein co-localization appear as yellow / orange.

For SDS PAGE and immunoblotting, cells were plated at 5 x 10^5 cells / cm^2 and treated with drugs at the indicated concentrations and after the indicated time of treatment, lysed in whole-cell lysis buffer (0.5 M Tris-HCl, pH 6.8, 2%SDS, 10% glycerol, 1% β-mercaptoethanol, 0.02% bromophenol blue), and the samples were boiled for 30 min. The boiled samples were loaded onto 10-14% SDS-PAGE and electrophoresis was run overnight. Proteins were electrophoretically transferred onto 0.22 μm nitrocellulose, and immunoblotted with various primary antibodies against different proteins. Immunoblots were visualized by an Odyssey infra red imaging system. For presentation, immunoblots after scanning were processed using Adobe PhotoShop CS2 and Figures generated in MicroSoft PowerPoint.

Infection of cells with recombinant adenoviruses. Cells were plated at 3 x 10^3 per cm^2 in each well of a into 8 chambered glass slide, a 12 well, a 6 well or a 60 mm plate. After plating (24h), cells were infected (hepatoma and pancreatic carcinoma cells; at a multiplicity of infection of 50) with a control empty vector virus (CMV) and adenoviruses to express activated caMEK1, activated caAKT, dominant negative dnAKT, dominant negative dnMEK1, the caspase 8 inhibitor CRM A, dominant negative caspase 9, c-FLIP-s, BCL-XL, or XIAP (Vector Biolabs, Philadelphia, PA). After infection (24h) cells were treated with the indicated concentrations of vorinostat or Na valproate / sorafenib and/or other drugs, and cell survival or changes in expression / phosphorylation determined 0-96h after drug treatment by trypan blue / TUNEL / flow cytometry assays and immunoblotting, respectively.

Molecular Pharmacology Fast Forward. Published on May 29, 2009 as DOI: 10.1124/mol.109.056309
This article has not been copyedited and formatted. The final version may differ from this version.

Transfection of cells with siRNA or with plasmids. For Plasmids: Cells were plated as described above and 24h after plating, transfected. For mouse embryonic fibroblasts (2-5μg) or other cell types (0.5μg) plasmids expressing a specific mRNA (or siRNA) or appropriate vector control plasmid DNA was diluted in 50μl serum-free and antibiotic-free medium (1 portion for each sample). Concurrently, 2μl Lipofectamine 2000 (Invitrogen), was diluted into 50μl of serum-free and antibiotic-free medium (1 portion for each sample). Diluted DNA was added to the diluted Lipofectamine 2000 for each sample and incubated at room temperature for 30 min. This mixture was added to each well / dish of cells containing 200μl serum-free and antibiotic-free medium for a total volume of 300 μl, and the cells were incubated for 4 h at 37 °C. An equal volume of 2x medium was then added to each well. Cells were incubated for 24h, then treated with vorinostat / sorafenib.

Transfection with siRNA: Cells were plated in 60 mm dishes from a fresh culture growing in log phase as described above, and 24h after plating transfected. Prior to transfection, the medium was aspirated and 1 ml serum-free medium was added to each plate. For transfection, 10 nM of the annealed siRNA, the positive sense control doubled stranded siRNA targeting GAPDH or the negative control (a "scrambled" (siSCR) sequence with no significant homology to any known gene sequences from mouse, rat or human cell lines) were used. Ten nM siRNA (scrambled or experimental for knock down) was diluted in serum-free media. Four μl Hiperfect (Qiagen) was added to this mixture and the solution was mixed by pipetting up and down several times. This solution was incubated at room temp for 10 min, then added dropwise to each dish. The medium in each dish was swirled gently to mix; then incubated at 37 ^{o}C for 2h. One ml of 10% (v/v) serum-containing medium was added to each plate, and cells were incubated at 37 ^{o}C for 36h before treatment with vorinostat / sorafenib (0-96h). Trypan blue exclusion / TUNEL / flow cytometry assays and SDSPAGE/immunoblotting analyses were performed at the indicated time points in each Figure.

Isolation of a crude cytosolic fraction. A crude membrane fraction was prepared from treated cells. Briefly, cells were washed twice in ice cold isotonic HEPES buffer (10 mM HEPES pH 7.5, 200 mM mannitol, 70 mM

sucrose, 1 μM EGTA, 10 μM protease inhibitor cocktail (Sigma, St. Louis, MO). Cells on ice were scraped into isotonic HEPES buffer and lysed by passing 20 times through a 25 gauge needle. Large membrane pieces, organelles and unlysed cells were removed from the suspension by centrifugation for 5 min at 120 x g. The crude granular fraction and cytosolic fraction was obtained from by centrifugation for 30 min at 10,000 x g, leaving the cytosol as supernatant.

Data analysis. Comparison of the effects of various treatments was performed using ANOVA and the Student's t test. Differences with a *p*-value of < 0.05 were considered statistically significant. Experiments shown are the means of multiple individual points (± SEM). Median dose effect isobologram analyses to determine synergism of drug interaction were performed according to the Methods of T.-C. Chou and P. Talalay using the Calcusyn program for Windows (BIOSOFT, Cambridge, UK). Cells are treated with agents at a fixed concentration dose. A combination index (CI) value of less than 1.00 indicates synergy of interaction between the drugs; a value of 1.00 indicates additivity; a value of > 1.00 equates to antagonism of action between the agents.

Molecular Pharmacology Fast Forward. Published on May 29, 2009 as DOI: 10.1124/mol.109.056309
This article has not been copyedited and formatted. The final version may differ from this version.

Results.

Vorinostat (suberoylanilide hydroxamic acid, Zolinza™) is a hydroxamic acid HDACI that has shown preliminary pre-clinical evidence of activity in hepatoma and other malignancies with a C_{max} of ~9 μM; however, the agent has a very short half life in plasma and steady state drug levels in many patients are ~ 1 μM or less (Pang and Poon, 2007; Venturelli et al, 2007; Wise et al, 2007). Treatment of pancreatic tumor cells (PANC1, MiaPaca2, ASPC-1) with concentrations of vorinostat and sorafenib that are sustainable in patient serum resulted in a greater than additive increase in tumor cell killing as assessed by short-term death assays (nuclear fragmentation by Dapi stain; trypan blue exclusion) and a synergistic increase in killing assessed by colony formation assays performed using median dose effect isobologram analyses (Figures 1A-1C; Tables 1 and 2). Suppression of caspase 8 function, as well as expression of dominant negative caspase 9 or BCL-XL also blunted sorafenib and vorinostat lethality (Figure 1A). Similar data to those in human tumor cell lines were obtained using the rodent pancreatic tumor line PAN02 (Supplemental Figure 1).

Sorafenib and vorinostat, but not treatment with the individual drugs activated CD95 and caused formation of a death inducing signal complex (DISC) containing caspase 8, FAS associated death domain (FADD), ATG5 and Grp78/BiP (Figures 1D and 1E, and Supplemental Figure 2). The ability of sorafenib and vorinostat to kill pancreatic tumor cells was suppressed by constitutive expression of c-FLIP-s, by knock down of CD95, or by expression of dominant negative PKR-like endoplasmic reticulum kinase (PERK) (Figure 1F, Table 1; Supplemental Figures 2 and 3). Treatment of pancreatic tumor cells with sorafenib + HDACI enhanced phosphorylation of PERK and its substrate eIF2α and decreased expression of BID and c-FLIP-s (Supplemental Figure 3). Sodium valproate is an anti-convulsive drug that also has HDACI activity (Rodriguez-Menendez et al, 2008). A clinically relevant and sustainable concentration of sodium valproate enhanced sorafenib lethality in a synergistic fashion in pancreatic tumor cells derived from either humans or rodents as judged in short-term cell death assays and in median dose effect isobologram colony formation assays (Supplemental Figure 1 and Table 2).

Molecular Pharmacology Fast Forward. Published on May 29, 2009 as DOI: 10.1124/mol.109.056309
This article has not been copyedited and formatted. The final version may differ from this version.

Sorafenib is an inhibitor of RAF family protein kinases that regulate the ERK1/2 pathway as well as an inhibitor of class III receptor tyrosine kinases that regulate the PI3K-AKT pathway. Hence, we determined whether modulation ERK1/2 and/or AKT activity altered the lethality of sorafenib and vorinostat exposure. Expression of constitutively activated MEK1 EE suppressed sorafenib + HDACI lethality in pancreatic and liver cancer cells, and in hepatoma cells expression of activated AKT also suppressed drug lethality (Supplemental Figure 4). Expression of dominant negative MEK1 and dominant negative AKT, but not the individual activated kinase, was required to enhance the lethality of sorafenib+vorinostat exposure. Thus the regulation of sorafenib+HDACI lethality occurs via both the ERK1/2 and AKT pathways in pancreatic and liver cancer cells. The findings in Figure 1, Tables 1 and 2 and Supplemental Figures 1-4 demonstrate that sorafenib + HDACI exposure induces an endoplasmic reticulum stress response in pancreatic tumor cells that promotes tumor cell death.

CD95 is known to mediate pro-apoptotic signaling through its association with FADD, and FADD by binding to pro-caspase 8 promoting auto-catalytic activation of pro-caspase 8, in the DISC. To further examine the biology of CD95 signaling after drug treatment we performed immunohistochemistry (IHC) in permeabilized cells with confocal microscopic examination for the cellular localization of multiple extrinsic apoptosis pathway / autophagy / endoplasmic reticulum (ER) stress regulatory proteins. In permeabilized HEP3B cells 6h following sorafenib + vorinostat treatment, we noted by IHC that CD95 co-localized with: Grp78/BiP and ATG5 (Figures 2A and 2B (white arrows indicated protein co-localization)). We next attempted to confirm our findings using immunoprecipitation and IHC using expression of transfected fluorescent tagged proteins. Transfection of hepatoma cells with plasmids to express CD95- yellow fluorescent protein (YFP) in combination with a construct to express ATG5-cherry red or FADD- green fluorescent protein (GFP) in combination with a construct to express ATG5-cherry red demonstrated within 6h after drug exposure that CD95 became visibly punctuate and based on the merging of images from the confocal microscope, that CD95 became associated with both ATG5 and FADD (Figures 2C and 2D). In permeabilized HEP3B cells 6h following sorafenib + vorinostat treatment, we noted by IHC that CD95 co-localized with the ER associated

Molecular Pharmacology Fast Forward. Published on May 29, 2009 as DOI: 10.1124/mol.109.056309
This article has not been copyedited and formatted. The final version may differ from this version.

protein calnexin (Figure 2E). Collectively, our findings argue that sorafenib and HDACI treatment rapidly promote activation of CD95 at internal sites within a tumor cell, and that "activated" CD95 subsequently migrates to the plasma membrane.

Based on data showing that knock down of CD95 expression reduced sorafenib + vorinostat lethality, we next explored whether cells lacking CD95 were resistant to drug-induced killing and whether re-expression of CD95 enhanced drug lethality. HuH7 cells that lack CD95 expression were relatively resistant to the lethal effects of sorafenib + vorinostat exposure (Figures 3A and 3B). Transient re-expression of CD95 in HuH7, with a CD95-YFP construct, significantly enhanced sorafenib + vorinostat lethality (Figure 3C). Previously we demonstrated that over-expression of the BCL-2 family protein BCL-XL suppressed sorafenib + vorinostat –induced killing. Using transformed mouse embryonic fibroblasts deleted for specific toxic BH3 domain proteins we also found that loss of BAX and BAK expression profoundly reduced the toxic interaction between sorafenib + vorinostat and also between sorafenib and sodium valproate (Supplemental Figure 5). Based on these findings, we then explored whether drugs that block the interaction of toxic BH3 domain proteins with protective BCL-2 family members could enhance the lethality of sorafenib + HDACI treatment, and whether inhibitors of cytoprotective BCL-2 family proteins could restore drug-induced killing in a CD95 null / knocked down environment. This is of potential clinical importance because CD95 expression and functional signaling by this death receptor is often lost in the more advanced metastatic tumors.

Treatment of HEPG2 or HEP3B cells with a low concentration of the BCL-2 and BCL-XL antagonist HA14-1 significantly enhanced the lethal effects of the primary sorafenib + vorinostat treatment (Figure 3D). In HEPG2 cells expressing c-FLIP-s the lethality of sorafenib + vorinostat treatment was abolished, however, in the presence of HA14-1 a significant large portion of primary sorafenib + vorinostat –induced killing was regained regardless of c-FLIP-s levels (Figure 3E). This correlated with restoration of drug-induced cytochrome c release into the cytosol (Figure 3F). Furthermore, in CD95 null HuH7 cells HA14-1 co-exposure significantly enhanced sorafenib + vorinostat lethality (Figure 3G). The relative increase in cell killing caused by sorafenib +

Molecular Pharmacology Fast Forward. Published on May 29, 2009 as DOI: 10.1124/mol.109.056309
This article has not been copyedited and formatted. The final version may differ from this version.

vorinostat ± HA14-1 exposure was also reflected in the enhanced release of cytochrome c from the mitochondria into the cytosolic fraction (Figure 3H). The findings in HuH7 cells which lack endogenous CD95 protein expression are suggestive that even in the absence of CD95, disruption of BCL-2 family protective mechanisms facilitates sorafenib + vorinostat lethality.

We next determined whether a more clinically relevant BCL-2 family inhibitor, GX15-070 (Obatoclax, GX) that inhibits BCL-2, BCL-XL *and* MCL-1 function, and that is entering phase II trials, could promote sorafenib + HDACI killing. A 48h exposure of HEPG2 cells to 1 μM or 3 μM sorafenib resulted in modest increases in cell killing that became larger in cells exposed to 6 μM or 10 μM of the drug (Figure 4A). GX15-070 treatment in the clinically relevant 50-250 nM dose range caused similar amounts of cell death in short-term viability assays regardless of dose; approximately 7-10% above vehicle control levels. We noted that GX15-070 treatment abolished the modest levels of sorafenib –induced cell death in the 1-3 μM dose range, and blunted the lethality of higher dose sorafenib, with an interaction that was less than additive (Figure 4A). GX15-070 treatment did not significantly enhance as single agents the amount of cell killing caused by the HDACIs vorinostat or sodium valproate in our cell system (Figure 4B). However, GX15-070 treatment significantly enhanced the level of killing caused by sorafenib+valproate exposure (Figures 4C and 4D). GX15-070 as a single agent activated BAX and did not appear to further enhance sorafenib+valproate –induced BAX activation (Figure 4E). GX15-070 as a single agent also activated BAK, and interacted in at least an additive fashion with sorafenib+valproate treatment to cause further BAK activation. In a similar manner to sorafenib+vorinostat exposure, these findings also correlated with sorafenib+valproate –inducing decreased expression of protective BCL-2 family proteins (Figure 4F). Unlike sorafenib+valproate treatment, GX15-070 as a single agent did not alter BCL-2 family protein expression and did not appear to further reduce BCL-2 family protein expression in the presence of sorafenib+HDACI (data not shown).

Molecular Pharmacology Fast Forward. Published on May 29, 2009 as DOI: 10.1124/mol.109.056309
This article has not been copyedited and formatted. The final version may differ from this version.

We next determined, in a manner similar to HA14-1, whether GX15-070 could restore drug-induced lethality in a cellular environment lacking CD95 death receptor signaling. The lethality of sorafenib + valproate exposure was blocked by over-expression of c-FLIP-s or knock down of CD95 in short-term viability assays (Figures 5A and 5B). GX15-070 enhanced sorafenib + valproate lethality and abolished the protective effect caused by either over-expression of c-FLIP-s or knock down of CD95. This effect was also observed in long-term colony formation assays in PANC-1 cells (Table 3, data not shown). The restoration of drug –induced lethality correlated with restoration of cytochrome c release into the cytosol in cells treated with GX15-070 and with sorafenib+HDACI+GX15-070 (Figure 5C). Enhanced sorafenib + valproate lethality correlated with reduced co-immunoprecipitation of toxic BH3 domain proteins with MCL-1 (Figure 5D). Of particular note, BAK association with MCL-1 was reduced within 6h of drug exposure, prior to any reduction in BCL-2 family protein levels, that correlated with activation of CD95 / caspase 8 and loss of full length BID expression (Figure 5D and Supplemental Figure 3). In parallel to these events, sorafenib+valproate treatment caused increased association of BAK and BAX with mitochondria and a reduction in the levels of these proteins in the cytosol (Figure 5E). Similar apoptosis and blotting data to that observed in hepatoma cells were also obtained in pancreatic tumor cells (Figures 6A and 6B; data not shown).

GX15-070 is an inhibitor of BCL-2, BCL-XL and MCL-1 function, whereas HA14-1 is an inhibitor of only BCL-2 and BCL-XL function, and we next determined whether individual or combined molecular knock down of these BCL-2 family proteins resulted in enhanced sorafenib + valproate lethality (Nguyan et al, 2007; Konopleva et al, 2008; Chen et al, 2007). Knock down of BCL-2 or BCL-XL or MCL-1 modestly though significantly enhanced sorafenib + valproate lethality (Figure 6C). Knock down of BCL-2 and BCL-XL to mimic the actions of HA14-1 or knock down of BCL-2, BCL-XL and MCL-1 to mimic the actions of GX15-070 caused significantly greater enhancements of sorafenib + valproate lethality than knock down of any individual BCL-2 family protein. Based on an additive summation of enhanced cell killing due to individual BCL-2 family protein knock down, we would have predicted that knock down of BCL-2 and BCL-XL would have elevated sorafenib+HDACI lethality by an additional 13.5% above control value whereas in fact we

Molecular Pharmacology Fast Forward. Published on May 29, 2009 as DOI: 10.1124/mol.109.056309
This article has not been copyedited and formatted. The final version may differ from this version.

observed a 23.0% increase above control ($p < 0.05$). We would have predicted that knock down of BCL-2, BCL-XL and MCL-1 would have elevated drug lethality by an additional 22.0% based on the additive effect of each individual knock down, whereas we observed a 31.5% increase ($p < 0.05$). These findings suggest that the major targets of HA14-1 / GX15-070 action when combined with sorafenib + valproate are BCL-2 / BCL-XL rather than MCL-1. In partial agreement with our data in transformed MEFs and with data in Figures 4 and 5, combined knock down of BAX and BAK expression modestly suppressed sorafenib+valproate killing in HEPG2 cells (Figure 6D). However, knock down of BAX and BAK expression almost abolished the ability of GX15-070 to promote sorafenib+valproate –induced tumor cell death.

Type II programmed cell death, also called autophagy, is a ubiquitous process that occurs in all eukaryotes. It is morphologically distinct from apoptosis, a different complement of proteins is activated, and, unlike apoptosis, may occur under both normal and stressed growth conditions. Autophagy is an apparently non-selective process in which cytoplasm and organelles are randomly assorted into the autophagosome, where they are degraded. The autophagic process is activated by both extracellular (starvation, hormone treatment, chemotherapy) and intracellular stimuli (e.g. accumulation of unfolded proteins in the ER). Studies from this laboratory have demonstrated that sorafenib + HDACI treatment causes a CD95-dependent form of autophagy; an autophagy that was protective against CD95-induced activation of caspase 8 as judged by knock down of either ATG5 or Beclin1 (Figure 7A) (Park et al., 2008a). Knock down of Beclin1 also suppressed the lethality of GX15-070 as a single agent and the ability of GX15-070 to enhance sorafenib + HDACI –induced killing, regardless of CD95 expression (Figure 7B). Both sorafenib + HDACI and GX15-070 treatments increased the vesicularization of a transfected LC3 (ATG8) – GFP construct, indicative of autophagy; and combined exposure to all three drugs further increased the number of vesicles present in each cell in at least an additive fashion (Figure 7C). Knock down of Beclin1 suppressed the ability of all tested drug combinations to increase autophagic vesicle levels. Knock down of BAX and BAK also suppressed GX15-070+sorafenib+valproate –induced autophagy (Figure 7D). Collectively, the data in Figures 6 and 7 argues that sorafenib + HDACI treatment causes a protective form of autophagy but that exposure to GX15-070, either as a single agent or in

Molecular Pharmacology Fast Forward. Published on May 29, 2009 as DOI: 10.1124/mol.109.056309
This article has not been copyedited and formatted. The final version may differ from this version.

combination with that sorafenib + HDACI treatment, promotes tumor cell killing in part by *elevating* levels of a lethal form of autophagy.

Molecular Pharmacology Fast Forward. Published on May 29, 2009 as DOI: 10.1124/mol.109.056309
This article has not been copyedited and formatted. The final version may differ from this version.

Discussion

We have attempted to determine in pancreatic tumor cells whether sorafenib and vorinostat interact synergistically to cause cell death, and whether inhibition of mitochondrial BCL-2 family protective protein association with toxic BH3 domain proteins could enhance sorafenib + HDACI lethality in the absence of CD95 / death receptor signaling.

The results of the present study indicate that low concentrations of sorafenib and vorinostat interact in a synergistic manner to kill pancreatic cancer cells in vitro. The enhanced lethality of the regimen toward multiple pancreatic cancer cells was also blocked by inhibition of CD95 function and abolished by over-expression of c-FLIP-s. Of particular note, use of a chemically unrelated HDACI sodium valproate, that is a widely used generic drug, enhanced the lethality of sorafenib in a near identical fashion to that of vorinostat, and synergized with sorafenib to kill liver and pancreatic tumor cells. Expression of CD95 enhanced drug-induced cell lethality in hepatoma cells lacking endogenous CD95. Collectively, our present findings argue that pancreatic tumor cells are susceptible to being rapidly killed by sorafenib + HDACI exposure through a death receptor / extrinsic pathway -dependent mechanism.

Studies in hepatoma and pancreatic cancer cells treated with sorafenib+vorinostat demonstrated that activated CD95 co-immunoprecipitated with regulators of both apoptosis, e.g. FADD, caspase 8, as well as regulators of ER stress signaling and autophagy, e.g. ATG5, Grp78/BiP. Recent studies from other groups have also argued that CD95 / death receptor signaling regulates a protective form of autophagy (Wang et al., 2008; Han et al, 2008). Knock down of caspase 8 expression can promote a toxic form of autophagy and in some systems, and treatment of cells with the pan-caspase inhibitor zVAD causes an autophagic form of cell death (Barnhart et al, 2003; Pyo et al, 2005). In our cells zVAD did not cause autophagic cell death (Unpublished data). FADD has previously been shown to co-localize with ATG5, and our present data are in agreement with these findings, although in the prior study interferon-induced FADD-ATG5 signaling in immune cells caused a pro-death autophagy signal (Barnhart et al, 2003; Petak et al, 2001; Park et al, 2005). It is well known that autophagy can

Molecular Pharmacology Fast Forward. Published on May 29, 2009 as DOI: 10.1124/mol.109.056309
This article has not been copyedited and formatted. The final version may differ from this version.

promote survival or death based on the cell stressing agent, the cell system being examined and the cell culture conditions, and the findings in hematopoietic cells with FADD promoting toxic autophagy suggest that in addition to our own data, it could be probable that death receptor / FADD / caspase 8 / FLIP –regulated autophagy will, under some circumstances, also play a role in toxic forms of autophagy (Han et al, 2008).

An inability to express death receptors or to over-express dominant negative acting forms of death receptors has been linked to apoptosis resistance (Dent et al., 2009; Park et al, 2005; Walsh et al, 2003). HuH7 cells lack CD95 expression and were particularly resistant to sorafenib + HDACI lethality compared to HEPG2 and HEP3B cells that express CD95. Re-expression of CD95 in HuH7 cells facilitated their killing after drug exposure. An additional mechanism that could block toxic death receptor signaling is constitutive high levels of c-FLIP-s. Over-expression of c-FLIP-s protected tumor cells from sorafenib + HDACI –induced tumor cell killing in short term and long term viability assays. We determined that small molecule antagonists of BCL-2 family proteins (HA14-1; GX15-070) enhanced sorafenib+HDACI lethality, and in cells over-expressing c-FLIP-s, or where death receptor signaling was suppressed by knock down of CD95 expression, HA14-1 or Obatoclax were capable of reverting sorafenib+HDACI lethality to levels approaching those in vector / siScrambled control cells. Sorafenib + vorinostat treatment activated multiple toxic BH3 domain proteins in cells, including BAX, BAK, BID and BIM, that in the case of BAK was further enhanced in the presence of GX15-070. Thus promoting a partial activation of the intrinsic apoptosis pathway by use of small molecule antagonists of BCL-2 family protein function; permitted sorafenib+HDACI exposure to cause cell killing independently of death receptor functionality, via the intrinsic pathway.

Prior studies have shown that sorafenib + vorinostat exposure increased the numbers of autophagic vesicles in tumor cells in a CD95- and PERK-dependent fashion, and that this form of autophagy was protective against CD95-induced activation of caspase 8 / caspase 3 and apoptosis (Park et al, 2008a). The Czaja laboratory recently demonstrated that autophagy induced from death receptor activation is a protective event whereas autophagy induced from mitochondrial dysfunction is a toxic event (Wang et al., 2008). Others have also shown

Molecular Pharmacology Fast Forward. Published on May 29, 2009 as DOI: 10.1124/mol.109.056309
This article has not been copyedited and formatted. The final version may differ from this version.

that death receptor signaling promotes a protective form of autophagy (Han et al., 2008). The BCL-2 / BCL-XL inhibitor ABT-737 has been shown to promote autophagy in tumor cells and we investigated whether the BCL-2 / BCL-XL / MCL-1 inhibitor also induced autophagy and whether this played a role in the survival of sorafenib + HDACI treated cells (Sandoval et al., 2008). Sorafenib + HDACI, GX15-070 and combined exposure to all three drugs increased the vesicularization of a transfected LC3 (ATG8) – GFP construct in a Beclin1- and BAX+BAK-dependent fashion, indicative of autophagy. Knock down of Beclin1 enhanced the ability of sorafenib + HADCI exposure to kill tumor cells whereas loss of Beclin1 expression suppressed the ability of GX15-070 as a single agent or when in combination with sorafenib + HDACI to cause cell death. Knock down of BAX+BAK modestly suppressed Sorafenib + HDACI lethality but abolished the ability of GX15-070 to restore "two drug" lethality. Thus GX15-070 reverts the apoptosis resistant phenotype in our CD95 knock down cell systems through increased toxic autophagy which requires BAX and BAK function, but in cells that contain a functional extrinsic pathway it does so by simultaneously overwhelming a protective CD95-dependent form of autophagy via a toxic mitochondrial form of autophagy. This data further underscores the essential need for a detailed molecular understanding how any drug combination kills tumor cells.

Sorafenib+HDACI exposure abolished MCL-1 expression within 24h and reduced expression of BCL-2 and BCL-XL. Knock down of individual and combinations of BCL-2 family proteins revealed that loss of BCL-2 and BCL-XL expression increased sorafenib+HDACI lethality in a greater than additive manner compared to the summation of individual effects. In contrast, loss of BCL-2, BCL-XL *and also* MCL-1 resulted in a potentiation of killing that was approximately additive between the effects caused by BCL-2 and BCL-XL knock down and MCL-1 knock down. Sorafenib as a single agent at higher concentrations induces ER stress signaling with resultant eIF2α-dependent translational repression and a lowering in the expression of short lived proteins such as MCL-1 (Rahmani et al, 2005). Thus a likely reason for our findings with respect to the relative impact of BCL-2 and BCL-XL protein knock down on sorafenib+HDACI –induced tumor cell killing may be due to the greater reduction of short-lived MCL-1 expression caused by sorafenib+HDACI exposure.

Sorafenib+HDACI exposure leads to CD95/caspase 8 activation, causing BID cleavage. Cleaved BID as a BH3 only domain protein can act to displace BAX, BAK and BIM from protective BCL-2 family proteins resulting in homo-oligomerization of BAK and possible association with BAX, resulting in mitochondrial pore formation and release of cytochrome c into the cytosol. The finding that GX15-070 as a single agent induced BAX, and to a lesser extent BAK, conformational change but only weakly triggered apoptosis by itself suggests that the lethality of the (sorafenib+HDACI) + GX15-070 regimen involves not simply activation of either BAX or BAK, but a cooperative interaction between these proteins, together with the loss of protective BCL-2 family protein levels. The notion of cooperative BAX and BAK actions in the regulation of sorafenib+HDACI lethality is further supported by the results obtained in BAX-/-, BAK-/- and BAX-BAK-/- transformed MEFs, as well as using siRNA knock down of BAX+BAK in hepatoma cells. BAX-/- MEFs were more resistant to sorafenib+HDACI lethality than BAK-/- cells; however, deletion of both proteins abolished drug lethality in MEFs and siRNA knock down partially reduced sorafenib+HDACI lethality in hepatoma cells. As sorafenib+vorinostat therapy is about to be explored in a phase I trial in hepatoma, our data suggest that the incorporation of GX15-070 (Obatoclax) together with sorafenib+HDACI therapy may provide significant additional value in tumor control, including tumors that lack extrinsic pathway signaling.

In conclusion, the results of the present study indicate that sorafenib and multiple HDACIs interact in a highly synergistic manner to kill pancreatic tumor cells in vitro via activation of CD95. These effects are magnified when BCL-2 family protein activity is inhibited and, of novelty, demonstrate that loss of extrinsic pathway activation which blocks cell killing is circumvented by use of a small molecule BCL-2 inhibitor, which restores drug –induced cell killing in part through toxic autophagy. Ongoing in vitro and future animal studies will be required to fully define the importance of sorafenib and vorinostat (or other HDACIs) as a therapeutic in cancer.

References.

Allan LA, Morrice N, Brady S, Magee G, Pathak S, Clarke PR. (2003) Inhibition of caspase-9 through phosphorylation at Thr 125 by ERK MAPK. *Nat Cell Biol* **5**:647–54.

Azmi AS, Mohammad RM. (2009) Non-peptidic small molecule inhibitors against Bcl-2 for cancer therapy. *J Cell Physiol.* **218**: 13-21.

Bali P, Pranpat M, Swaby R, et al. (2005) Activity of suberoylanilide hydroxamic Acid against human breast cancer cells with amplification of her-2. *Clin Cancer Res* **11**: 6382-9.

Bardeesy N, DePinho RA. (2002) Pancreatic cancer biology and genetics. *Nat Rev Cancer* **2**: 897–909.

Barnhart BC, Alappat EC, Peter ME. (2003) The CD95 type I/type II model. *Semin Immunol* **15**:185-93.

Chen S, Dai Y, Harada H, Dent P, Grant S. (2007) Mcl-1 down-regulation potentiates ABT-737 lethality by cooperatively inducing Bak activation and Bax translocation. *Cancer Res.* **67**: 782-91

Dai Y, Grant S. (2007) Targeting multiple arms of the apoptotic regulatory machinery. *Cancer Res.* **67**: 2908-11.

Dasmahapatra G, Yerram N, Dai Y, Dent P, Grant S. (2007) Synergistic interactions between vorinostat and sorafenib in chronic myelogenous leukemia cells involve Mcl-1 and p21CIP1 down-regulation. *Clin Cancer Res* **13**:4280-90.

Davies BR, Logie A, McKay JS, et al. (2007) AZD6244 (ARRY-142886), a potent inhibitor of mitogen-activated protein kinase/extracellular signal-regulated kinase kinase 1/2 kinases: mechanism of action in vivo, pharmacokinetic/pharmacodynamic relationship, and potential for combination in preclinical models. *Mol Cancer Ther* **6**:2209-19.

Dent P, Yacoub A, Fisher PB, Hagan MP, Grant S. (2003) MAPK pathways in radiation responses. *Oncogene* **22**:5885-96.

Dent, P. (2005) *MAP kinase pathways in the control of hepatocyte growth, metabolism and survival.* Signaling Pathways in Liver Diseases, Springer Press. Chapter 19. pp 223-238 Eds. J.F. Dufour P.-A. Clavien.

Dent P, Curiel DT, Fisher PB, Grant S. (2009) Synergistic combinations of signaling pathway inhibitors: Mechanisms for improved cancer therapy. *Drug Resist Updat.* Apr 21. [Epub ahead of print]

Flaherty KT. (2007) Sorafenib: delivering a targeted drug to the right targets. *Expert Rev Anticancer Ther* **7**:617-26.

Gollob JA. (2005) Sorafenib: scientific rationales for single-agent and combination therapy in clear-cell renal cell carcinoma. *Clin Genitourin Cancer* **4**:167-74.

Grant S, Dent P. (2004) Kinase inhibitors and cytotoxic drug resistance. *Clin Cancer Res* **10**:2205-7.

Gregory P. D., Wagner K., Horz W. (2001) Histone acetylation and chromatin remodeling. *Exp. Cell Res* **265**: 195-202.

Han J, Hou W, Goldstein LA, Lu C, Stolz DB, Yin XM, Rabinowich H. (2008) Involvement of protective autophagy in TRAIL resistance of apoptosis-defective tumor cells. *J Biol Chem.* **283**: 19665-77.

Kang MH, Reynolds CP. (2009) Bcl-2 inhibitors: targeting mitochondrial apoptotic pathways in cancer therapy. *Clin Cancer Res.* **15**:1126-32.

Kim SH, Ricci MS, El-Deiry WS. (2008) Mcl-1: a gateway to TRAIL sensitization. *Cancer Res.* **68**: 2062-4.

Konopleva M, Watt J, Contractor R, Tsao T, Harris D, Estrov Z, Bornmann W, Kantarjian H, Viallet J, Samudio I, Andreeff M. (2008) Mechanisms of antileukemic activity of the novel Bcl-2 homology domain-3 mimetic GX15-070 (obatoclax). *Cancer Res.* **68**: 3413-20.

Kwon SH, Ahn SH, Kim YK, et al. (2002) Apicidin, a histone deacetylase inhibitor, induces apoptosis and Fas/Fas ligand expression in human acute promyelocytic leukemia cells. *J Biol Chem* **277**: 2073-80.

Lessene G, Czabotar PE, Colman PM. (2008) BCL-2 family antagonists for cancer therapy. *Nat Rev Drug Discov.* **7**:989-1000.

Ley R, Balmanno K, Hadfield K, Weston C, Cook SJ. (2003) Activation of the ERK1/2 signaling pathway promotes phosphorylation and proteasome-dependent degradation of the BH3-only protein, Bim. *J Biol Chem* **278**:18811–6.

Li N, Batt D, Warmuth M. (2007) B-Raf kinase inhibitors for cancer treatment. *Curr Opin Investig Drugs* **8**:452-6.

Marks PA, Miller T, and Richon VM. (2003) Histone deacetylases. *Curr Opin Pharmacol* **3**: 344-351.

Mitchell C, Park MA, Zhang G, Han SI, Harada H, Franklin RA, Yacoub A, Li PL, Hylemon PB, Grant S, Dent P. (2007) 17-Allylamino-17-demethoxygeldanamycin enhances the lethality of deoxycholic acid in primary rodent hepatocytes and established cell lines. *Mol Cancer Ther* **6**: 618-32.

Mori M, Uchida M, Watanabe T, et al. (2003) Activation of extracellular signal-regulated kinases ERK1 and ERK2 induces Bcl-xL up-regulation via inhibition of caspase activities in erythropoietin signaling. *J Cell Physiol* **195**:290–7.

Nguyen M, Marcellus RC, Roulston A, Watson M, Serfass L, Murthy Madiraju SR, Goulet D, Viallet J, Bélec L, Billot X, Acoca S, Purisima E, Wiegmans A, Cluse L, Johnstone RW, Beauparlant P, Shore GC. (2007) Small molecule obatoclax (GX15-070) antagonizes MCL-1 and overcomes MCL-1-mediated resistance to apoptosis. *Proc Natl Acad Sci U S A.* **104**: 19512-7.

Pang RW, Poon RT. (2007) From molecular biology to targeted therapies for hepatocellular carcinoma: the future is now. *Oncology* **72 S1** 1: 30-44.

Park MA, Zhang G, Martin AP, Hamed H, Mitchell C, Hylemon PB, Graf M, Rahmani M, Ryan K, Liu X, Spiegel S, Norris J, Fisher PB, Roberts JD, Grant S, Dent P. (2008a) Vorinostat and sorafenib increase ER stress, autophagy and apoptosis via ceramide-dependent CD95 and PERK activation. *Cancer Biol & Ther* **7**: 135-149.

Park MA, Yacoub A, Rahmani M, et al. (2008b) OSU-03012 stimulates PERK-dependent increases in HSP70 expression, attenuating its lethal actions in transformed cells. *Mol Pharmacol* **73**: 1168-84.

Park MA, Zhang G, Mitchell C, Rahmani M, Hamed H, Hagan MP, Yacoub A, Curiel DT, Fisher PB, Grant S and Dent P. (2008c) Mitogen-activated protein kinase kinase 1/2 inhibitors and 17-allylamino-17-demethoxygeldanamycin synergize to kill human gastrointestinal tumor cells *in vitro* via suppression of c-FLIP-s levels and activation of CD95. *Mol Cancer Ther* **7**: 2633-2648.

Park SM, Schickel R, Peter ME. (2005) Non-apoptotic functions of FADD-binding death receptors and their signaling molecules. *Curr Opin Cell Biol* **17**: 610-6.

Parkin DM, Bray F, Ferlay J, Pisani P. (2005) Global cancer statistics, 2002. *CA Cancer J Clin* **55**:74–108.

Peták I, Houghton JA. (2001) Shared pathways: death receptors and cytotoxic drugs in cancer therapy. *Pathol Oncol Res* **7**: 95-106.

Peter ME, Budd RC, Desbarats J, Hedrick SM, Hueber AO, Newell MK, Owen LB, Pope RM, Tschopp J, Wajant H, Wallach D, Wiltrout RH, Zörnig M, Lynch DH. (2007) The CD95 receptor: apoptosis revisited. *Cell.* **129**: 447-50.

Pyo JO, Jang MH, Kwon YK, et al. (2005) Essential roles of Atg5 and FADD in autophagic cell death: dissection of autophagic cell death into vacuole formation and cell death. *J Biol Chem* **280**: 20722-9.

Qiao L, Studer E, Leach K, et al. (2001) Deoxycholic acid (DCA) causes ligand-independent activation of epidermal growth factor receptor (EGFR) and FAS receptor in primary hepatocytes: inhibition of EGFR/mitogen-activated protein kinase-signaling module enhances DCA-induced apoptosis. *Mol Biol Cell* **12**:2629-45.

Qiao L, Han SI, Fang Y, et al. (2003) Bile acid regulation of C/EBPbeta, CREB, and c-Jun function, via the extracellular signal-regulated kinase and c-Jun NH2-terminal kinase pathways, modulates the apoptotic response of hepatocytes. *Mol Cell Biol.* **23**:3052-66.

Rahmani M, Davis EM, Bauer C, Dent P, Grant S. (2005) Apoptosis induced by the kinase inhibitor BAY 43-9006 in human leukemia cells involves down-regulation of Mcl-1 through inhibition of translation. *J Biol Chem* **280**:35217-27.

Rahmani M, Nguyen TK, Dent P, Grant S. (2007a) The multikinase inhibitor sorafenib induces apoptosis in highly imatinib mesylate-resistant bcr/abl+ human leukemia cells in association with signal transducer and activator of transcription 5 inhibition and myeloid cell leukemia-1 down-regulation. *Mol Pharmacol* **72**:788-95.

Rahmani M, Davis EM, Crabtree TR, et al. (2007b) The kinase inhibitor sorafenib induces cell death through a process involving induction of endoplasmic reticulum stress. *Mol Cell Biol.* **27**:5499-513.

Rini BI. (2006) Sorafenib. *Expert Opin Pharmacother.* **7**:453-61.

Rodriguez-Menendez V, Tremolizzo L, Cavaletti G. (2008) Targeting cancer and neuropathy with histone deacetylase inhibitors: two birds with one stone? *Curr Cancer Drug Targets.* **8**:266-74.

Sandoval H, Thiagarajan P, Dasgupta SK, Schumacher A, Prchal JT, Chen M, Wang J. (2008) Essential role for Nix in autophagic maturation of erythroid cells. *Nature.* **454**: 232-5.

Strumberg D. (2005) Preclinical and clinical development of the oral multikinase inhibitor sorafenib in cancer treatment. *Drugs Today (Barc)* **41**:773-84.

Susnow N, Zeng L, Margineantu D, Hockenbery DM. (2009) Bcl-2 family proteins as regulators of oxidative stress. *Semin Cancer Biol.* **19**:42-9.

Valerie K, Yacoub A, Hagan MP, et al. (2007) Radiation-induced cell signaling: inside-out and outside-in. *Mol Cancer Ther* **6**:789-801.

Venturelli S, Armeanu S, Pathil A, et al. (2007) Epigenetic combination therapy as a tumor-selective treatment approach for hepatocellular carcinoma. *Cancer.* **109**: 2132-41.

Walsh CM, Luhrs KA, Arechiga AF. (2003) The "fuzzy logic" of the death-inducing signaling complex in lymphocytes. *J Clin Immunol.* **23**: 333-53.

Wang Y, Singh R, Massey AC, Kane SS, Kaushik S, Grant T, Xiang Y, Cuervo AM, Czaja MJ. (2008) Loss of macroautophagy promotes or prevents fibroblast apoptosis depending on the death stimulus. *J Biol Chem*. **283**: 4766-77.

Wang YF, Jiang CC, Kiejda KA, Gillespie S, Zhang XD, Hersey P. (2007) Apoptosis induction in human melanoma cells by inhibition of MEK is caspase-independent and mediated by the Bcl-2 family members PUMA, Bim, and Mcl-1. *Clin Cancer Res* **13**:4934-42.

Wise LD, Turner KJ, Kerr JS. (2007) Assessment of developmental toxicity of vorinostat, a histone deacetylase inhibitor, in Sprague-Dawley rats and Dutch Belted rabbits. *Birth Defects Res B Dev Reprod Toxicol* **80**: 57-68.

Yacoub A, Park MA, Gupta P, et al. (2008) Caspase-, cathepsin- and PERK-dependent regulation of MDA-7/IL-24-induced cell killing in primary human glioma cells. *Mol Cancer Ther* **7**: 297-313.

Zhang G, Park M, Mitchell C, et al. (2008) Vorinostat and sorafenib synergistically kill tumor cells via FLIP suppression and CD95 activation. *Clin Cancer Res* **14**: 5385-99.

Zhang L, Ming L, Yu J. (2007) BH3 mimetics to improve cancer therapy; mechanisms and examples. *Drug Resist Updat.* **10**: 207-17.

Footnotes.

*These authors contributed equally to the studies in this manuscript.

This work was funded from Public Health Service grants [R01-DK52825, P01-CA104177, R01-CA108520, R01-CA63753; R01-CA77141]. These studies were also funded in part by The Jimmy V Foundation and by The Goodwin Foundation for Cancer Research (to Massey Cancer Center). PD is the holder of the Universal Inc. Professorship in Signal Transduction Research.

Molecular Pharmacology Fast Forward. Published on May 29, 2009 as DOI: 10.1124/mol.109.056309
This article has not been copyedited and formatted. The final version may differ from this version.

Legends for Figures.

Figure 1. Sorafenib and Vorinostat interact in a synergistic fashion to kill pancreatic cancer cells via the death receptor CD95. Panel A. MiaPaca2 cells were infected with the indicated recombinant adenoviruses. Cells were treated with vehicle, sorafenib, vorinostat or sorafenib + vorinostat as per Methods. Cells were isolated after 96h and viability determined by trypan blue assay (n = 3, ± SEM) # $p < 0.05$ less cell killing than compared to parallel condition in vehicle treatment cells. **Panels B.** and **C.** MiaPaca2, PANC1 and AsPC1 cells were infected with the indicated recombinant adenoviruses and subsequently treated with vehicle, sorafenib, vorinostat or sorafenib + vorinostat. Cells were isolated 48h later and viability determined using: MiaPaca2 and AsPC1 cells, trypan blue exclusion (± SEM, n = 3). # $p < 0.05$ less than corresponding value in CMV vector cells; PANC1 cells, DAPI to examine nuclear morphology. Pictorial data are from a representative study (n = 3, ± SEM). * $p < 0.01$ greater than vehicle control; # $p < 0.01$ less than corresponding value in CMV infected cells. **Panel D.** HEPG2 and PANC1 cells were treated with vehicle, vorinostat, sodium valproate, sorafenib, sorafenib+vorinostat or sorafenib+valproate. After treatment (6h) cells were fixed but not permeabilized. Cells were stained with anti-CD95 antibody and visualized with an FITC secondary antibody at 40X magnification. Data are a representative study (± SEM n = 3 for CD95 quantitation). **Panel E.** PANC1 cells were treated with vehicle, vorinostat, sorafenib or sorafenib+vorinostat. Six h after exposure, cells were lysed and CD95 immunoprecipitated to determine the presence of indicated associated proteins in the DISC. **Panel F.** PANC-1 cells were transfected with siRNA molecules and subsequently treated with vehicle, vorinostat, sorafenib or sorafenib+vorinostat. Forty eight h after drug exposure cell viability determined using a trypan blue exclusion assay (± SEM, n = 3). # $p < 0.05$ less than corresponding value in CMV vector cells.

Figure 2. Sorafenib and HDACIs cause CD95 to associate with ER resident proteins that correlates with CD95 plasma membrane localization and DISC formation. Panel A. and Panel B. HEPG2 cells were treated with vehicle, vorinostat, sorafenib or sorafenib + vorinostat as per Methods. After drug treatment cells were fixed, permeabilized and stained with the indicated primary antibodies and visualized with secondary

Molecular Pharmacology Fast Forward. Published on May 29, 2009 as DOI: 10.1124/mol.109.056309
This article has not been copyedited and formatted. The final version may differ from this version.

antibodies with conjugated fluorescent probes (FITC, PE). Data are from a representative study (n = 3). **Panel C. and Panel D.** HEP3B cells were transfected as indicated with plasmids and subsequently were treated with vehicle, vorinostat, sorafenib or sorafenib+vorinostat. Six h after drug treatment cells were placed onto a confocal microscope stage and using appropriate filters, images of live cells captured at 40X magnification. Data in each panel are from a representative study (n = 3). **Panel E.** HEPG2 cells were treated with vehicle, vorinostat, sorafenib or sorafenib+vorinostat. Six h after drug treatment cells were fixed and permeabilized. Cells were stained with the indicated primary antibodies and visualized with secondary antibodies with conjugated fluorescent probes (FITC, PE). Cells were visualized using the appropriate fluorescent light filters at 40X. Data are from a representative study (n = 3).

Figure 3. The BCL-2/BCL-XL inhibitor HA14-1 promotes sorafenib+vorinostat -induced killing and circumvents the protective effects of either CD95 knock down or c-FLIP-s over-expression. Panel A. HuH7, HEPG2 and HEP3B cells were treated with vehicle, vorinostat, sorafenib or sorafenib+vorinostat. Forty eight h after drug exposure cell viability was determined using a TUNEL assay for DNA strand breaks (± SEM, n = 3). **Panel B.** Hepatoma cells were isolated 6h and 24h after drug exposure and immunoblotting performed to determine the expression of CD95 and GAPDH (a representative, n = 2-5). **Panel C.** HuH7 cells 24h after plating in triplicate were transfected with an empty vector plasmid (CMV) or a plasmid to express CD95-YFP and subsequently were treated with vehicle; sorafenib + vorinostat. Forty eight h after drug exposure cell viability determined by trypan blue exclusion assay (± SEM, n = 2). **Panel D.** HEPG2 and HEP3B cells were treated with vehicle, vorinostat, sorafenib or sorafenib+vorinostat, and in parallel with either vehicle or HA14-1. Twenty four h after exposure cell viability determined using trypan blue exclusion (± SEM, n = 2). # $p < 0.05$ greater than vehicle control; ## $p < 0.05$ greater than cells lacking HA14-1. **Panel E.** HEPG2 cells were infected with recombinant adenoviruses and were subsequently treated with vehicle, vorinostat, sorafenib or sorafenib+vorinostat, and in parallel with either vehicle (DMSO) or HA14-1. Twenty four h after exposure, cell viability was determined using TUNEL assays (± SEM, n = 2). * $p < 0.05$ less than corresponding value in

CMV vector cells; ## $p < 0.05$ greater than cells lacking HA14-1. **Panel F.** Parallel sets of infected cells to those in *Panel E.* were treated with drugs and 24h after exposure cell fractionation to isolate the crude granular and cytosolic fractions was performed to determine cytochrome c levels (n = 2). **Panel G.** HuH7 cells were infected with recombinant adenoviruses and subsequently treated with vehicle, vorinostat, sorafenib or sorafenib+vorinostat, and in parallel with either vehicle (DMSO) or HA14-1. Forty eight h after exposure, cell viability was determined using Annexin V – PI flow cytometry assays (± SEM, n = 2). ## $p < 0.05$ greater than cells lacking HA14-1. **Panel H.** Parallel sets of infected HuH7 cells were treated with drugs and 24h after exposure cell fractionation to isolate the crude granular and cytosolic fractions was performed to determine cytochrome c levels (n = 2).

Figure 4. Sorafenib and sodium valproate combination lethality is enhanced by GX15-070 (Obatoclax). **Panel A.** HEPG2 cells were treated with vehicle or GX15-070 in the presence or absence of sorafenib. Cells were isolated after 48h and viability determined using trypan blue exclusion (± SEM, n = 3). **Panel B.** HEPG2 cells were treated with vehicle or GX15-070 in the presence or absence of either vorinostat or sodium valproate. Cells were isolated after 48h and viability determined using trypan blue exclusion (± SEM, n = 3). **Panel C.** HEPG2 cells were treated with vehicle or GX15-070 in the presence or absence of sodium valproate and sorafenib. Cells were isolated 48h after exposure and viability determined using trypan blue exclusion (± SEM, n = 3). **Panel D.** HEPG2 cells were treated with vehicle or GX15-070 in the presence or absence of sorafenib and sodium valproate. Cells were isolated 24h and 48h after drug exposure and viability determined using trypan blue exclusion (± SEM, n = 3). **Panel E.** HEPG2 cells were treated with vehicle or GX15-070 in the presence or absence of sodium valproate and sorafenib. Twenty four h after treatment the activation of BAX and BAK was determined after immunoprecipitation (n = 3). **Panel F.** HEPG2 cells were treated with vehicle in the presence or absence of sodium valproate and/or sorafenib. Twenty four h after treatment cells the expression of BCL-2, BCL-XL and MCL-1 was determined by SDS PAGE / blotting (n = 3).

Molecular Pharmacology Fast Forward. Published on May 29, 2009 as DOI: 10.1124/mol.109.056309
This article has not been copyedited and formatted. The final version may differ from this version.

Figure 5. The BCL-2 / BCL-XL / MCL-1 inhibitor GX15-070 promotes sorafenib and valproate - induced killing and circumvents the protective effects of either CD95 knock down or c-FLIP-s over-expression. Panel A. HEPG2 cells were infected with recombinant adenoviruses and 24h after infection, cells were treated with vehicle, sodium valproate, sorafenib or sorafenib+valproate, and in parallel with either vehicle or GX15-070. Twenty four h after exposure, cell viability was determined using trypan blue exclusion assays (± SEM, n = 3). * $p < 0.05$ less than corresponding value in CMV vector cells; ## $p < 0.05$ greater than cells lacking GX15-070. **Panel B.** HEPG2 cells were transfected with siRNA to knock down CD95 (siCD95). Cells were treated 36h later with vehicle, sodium valproate, sorafenib or sorafenib+vorinostat, and in parallel with either vehicle or GX15-070. Twenty four h after drug exposure viability was determined using trypan blue exclusion (± SEM, n = 3). * $p < 0.05$ less than corresponding value in CMV vector cells; ## $p < 0.05$ greater than cells lacking GX15-070. **Panel C.** Parallel sets of HEPG2 cells from *Panel A.* were treated with drugs and 24h after exposure cell fractionation to isolate the crude granular and cytosolic fractions was performed to determine cytochrome c levels (n = 2). **Panel D.** HEPG2 cells were treated with vehicle, sodium valproate, sorafenib or sorafenib+vorinostat, and twelve hours after exposure equal portions of cell lysate subjected to immunoprecipitation for MCL-1 or for immunoblotting for total levels of BAK, BIM and MCL-1 (n = 2). **Panel E.** HEPG2 cells were treated with vehicle, sodium valproate, sorafenib or sorafenib+vorinostat and twelve hours after exposure cytosolic and crude granular fractions obtained by differential centrifugation. Equal protein equal portions of the lysate subjected SDS PAGE followed by immunoblotting to determine the total levels of BAK and BAX in each cell fraction (n = 2).

Figure 6. GX15-070 promotes sorafenib and valproate -induced killing in pancreatic cancer cells. Panel A. PANC1 cells were infected with recombinant adenoviruses and twenty four h after infection, cells were treated with vehicle, sodium valproate, sorafenib or sorafenib+valproate, and in parallel with either vehicle or GX15-070. Twenty four h after exposure, cell viability determined using trypan blue exclusion assays. **Panel B.** PANC1 cells were transfected with siRNA to knock down CD95 (siCD95). Thirty six h after transfection, cells were treated with vehicle, sodium valproate, sorafenib or sorafenib+vorinostat, and in parallel with either

Molecular Pharmacology Fast Forward. Published on May 29, 2009 as DOI: 10.1124/mol.109.056309
This article has not been copyedited and formatted. The final version may differ from this version.

vehicle or GX15-070. Twenty four h after exposure, cell viability was determined using a trypan blue exclusion assay (± SEM, n = 3). **Panel C.** HEPG2 cells were transfected with scrambled siRNA or transfected with siRNA molecules to knock down BCL-2, BCL-XL, MCL-1, BCL-2+BCL-XL or BCL-2+BCL-XL+MCL-1expression. Thirty six h after transfection, cells were treated with vehicle, valproate and sorafenib. Forty eight h after exposure, cell viability was determined using a trypan blue exclusion assay (± SEM, n = 4). # $p < 0.05$ greater than corresponding value in siSCR cells; ## $p < 0.05$ greater than cells with single knock down of a BCL-2 family protein. **Panel D.** HEPG2 cells were transfected with scrambled siRNA or transfected with siRNA molecules to knock down BAX and BAK. In parallel the cells were infected with empty vector virus (CMV) or a virus to express c-FLIP-s. Thirty six h after transfection, cells were treated with vehicle, valproate+sorafenib, GX15-070 or GX15-070+ valproate+sorafenib. Forty eight h after exposure, cell viability was determined using a trypan blue exclusion assay (± SEM, n = 2). * $p < 0.05$ less than corresponding value in siSCR cells.

Figure 7. GX15-070 promotes a toxic form of autophagy to facilitate sorafenib + HDACI killing. Panel A. HEPG2 cells were transfected with scrambled siRNA (siSCR) or transfected with siRNA molecules to knock down expression of ATG5, Beclin1 or CD95. Thirty six h after transfection, cells were treated with vehicle, vorinostat and sorafenib. Forty eight h after exposure, cell viability was determined using a trypan blue exclusion assay (± SEM, n = 2). # $p < 0.05$ greater than corresponding value in siSCR cells. **Panel B.** HEPG2 cells were transfected with scrambled siRNA (siSCR) or transfected with siRNA molecules to knock down expression of Beclin1 and/or CD95. Thirty six h after transfection, cells were treated with vehicle, GX15-070, valproate and sorafenib. Forty eight h after exposure, cell viability was determined using a trypan blue exclusion assay (± SEM, n = 2). * $p < 0.05$ less than corresponding value in siSCR cells; $ $p < 0.05$ greater than corresponding value in siSCR cells; # $p < 0.05$ less than corresponding value in siBeclin1 cells; ** $p > 0.05$ the corresponding value in siCD95 cells. **Panel C.** HEPG2 cells were transfected with a plasmid to express LC3-GFP and in parallel were transfected with scrambled siRNA (siSCR) or transfected with siRNA molecules to knock down expression of Beclin1. Thirty six h after transfection, cells were treated with vehicle, GX15-070,

valproate and sorafenib. Six h after exposure, the vesicularization of the LC3-GFP construct was determined using fluorescent microscopy (± SEM, n = 2) * $p < 0.05$ less than corresponding value in siSCR cells. **Panel D.** HEPG2 cells were transfected with a plasmid to express LC3-GFP and in parallel were transfected with scrambled siRNA (siSCR) or transfected with siRNA molecules to knock down expression of BAX and BAK. Thirty six h after transfection, cells were treated with vehicle, GX15-070, valproate and sorafenib. Six h after exposure, the vesicularization of the LC3-GFP construct was determined using fluorescent microscopy (± SEM, n = 2) * $p < 0.05$ less than corresponding value in siSCR cells.

Molecular Pharmacology Fast Forward. Published on May 29, 2009 as DOI: 10.1124/mol.109.056309
This article has not been copyedited and formatted. The final version may differ from this version.

Table 1. Sorafenib synergizes with vorinostat to kill pancreatic tumor cells that is abolished by over-expression of c-FLIP-s. Pancreatic cancer (Mia Paca 2; PANC1; AsPc1) and hepatoma (HEP3B) cells were infected 12h after plating at an approximate multiplicity of infection of 50 with either a control empty vector recombinant adenovirus (CMV) or a recombinant virus to express the caspase 8 inhibitor c-FLIP-s. Twenty four hours after infection, infected cells were plated as single cells (250-1500 cells/well) in sextuplicate and 12h after this plating the infected cells were treated with vehicle (VEH, DMSO), sorafenib (Sor., 3.0-6.0 μM) or vorinostat (Vor. 250-500 nM), or with both drugs combined, as indicated at a fixed concentration ratio to perform median dose effect analyses for the determination of synergy. After drug exposure (48h), the media was changed and cells cultured in drug free media for an additional 10-14 days. Cells were fixed, stained with crystal violet and colonies of > 50 cells / colony counted. Colony formation data were entered into the Calcusyn program and combination index (CI) values determined. A CI value of less than 1.00 indicates synergy.

Mia Paca2 : CMV

Sor (μM)	Vor (μM)	Fa	CI
3.00	0.250	0.34	0.32
4.50	0.375	0.42	0.40
6.00	0.500	0.50	0.45

Mia Paca2 : c-FLIP-s

Sor (μM)	Vor (μM)	Fa	CI
3.00	0.250	0.16	0.98
4.50	0.375	0.21	1.23
6.00	0.500	0.26	1.42

PANC1 : CMV

Sor (μM)	Vor (μM)	Fa	CI
3.00	0.250	0.22	0.38
4.50	0.375	0.28	0.42
6.00	0.500	0.36	0.38

PANC1 : c-FLIP-s

Sor (μM)	Vor (μM)	Fa	CI
3.00	0.250	0.06	0.92
4.50	0.375	0.10	1.00
6.00	0.500	0.15	1.03

AsPc1 : CMV

Sor (μM)	Vor (μM)	Fa	CI
3.00	0.250	0.34	0.34
4.50	0.375	0.48	0.40
6.00	0.500	0.58	0.45

AsPc1 : c-FLIP-s

Sor (μM)	Vor (μM)	Fa	CI
3.00	0.250	0.08	1.08
4.50	0.375	0.11	0.96
6.00	0.500	0.19	0.77

Hep3B : CMV

Sor (μM)	Vor (μM)	Fa	CI
3.0	0.250	0.43	0.47
4.5	0.375	0.56	0.58
6.0	0.500	0.74	0.58

Hep3B : c-FLIP-s

Sor (μM)	Vor (μM)	Fa	CI
3.0	0.250	0.26	0.90
4.5	0.375	0.40	0.97
6.0	0.500	0.54	1.08

Molecular Pharmacology Fast Forward. Published on May 29, 2009 as DOI: 10.1124/mol.109.056309
This article has not been copyedited and formatted. The final version may differ from this version.

Table 2. Sorafenib synergizes with sodium valproate to kill pancreatic and liver tumor cells Pancreatic cancer (Mia Paca2; PANC1) and hepatoma (HEP3B) cells 12h after plating were treated with vehicle (VEH, DMSO), sorafenib (Sor., 2.25-9.00 μM) or sodium valproate (Val. 0.50-1.50 mM), or with both drugs combined, as indicated at a fixed concentration ratio to perform median dose effect analyses for the determination of synergy. After drug exposure (48h), the media was changed and cells cultured in drug free media for an additional 10-14 days. Cells were fixed, stained with crystal violet and colonies of > 50 cells / colony counted. Colony formation data were entered into the Calcusyn program and combination index (CI) values determined. A CI value of less than 1.00 indicates synergy.

MiaPaca2			
Sor (μM)	Valproic (mM)	Fa	CI
2.25	0.75	0.35	0.82
3.00	1.00	0.46	0.73
3.75	1.25	0.54	0.65
HEP3B			
Sor (μM)	Valproic (mM)	Fa	CI
2.25	0.75	0.17	0.69
3.00	1.00	0.19	0.68
3.75	1.25	0.36	0.54
PANC1			
Sor (μM)	Valproic (mM)	Fa	CI
3.0	0.50	0.37	0.46
4.5	0.75	0.43	0.58
6.0	1.00	0.54	0.57
7.5	1.25	0.73	0.41
9.0	1.50	0.80	0.37

Molecular Pharmacology Fast Forward. Published on May 29, 2009 as DOI: 10.1124/mol.109.056309
This article has not been copyedited and formatted. The final version may differ from this version.

Table 3. Obatoclax restores the synergy of sorafenib+valproate toxicity in cells with blocked extrinsic pathway signaling. Pancreatic cancer (PANC1) cells were infected 12h after plating at an approximate multiplicity of infection of 50 with either a control empty vector recombinant adenovirus (CMV) or a recombinant virus to express the caspase 8 inhibitor c-FLIP-s. Twenty four hours after infection, infected cells were plated as single cells (250-1500 cells/well) in sextuplicate and 12h after this plating the infected cells were treated with vehicle (VEH, DMSO), sorafenib (Sor., 2.25 - 3.75 μM) or sodium valproate (Val. 0.75 - 1.25 mM), or with both drugs combined, as indicated at a fixed concentration ratio to perform median dose effect analyses for the determination of synergy. Cells were in parallel treated with either vehicle (DMSO) or Obatoclax (GX, 50 nM). After drug exposure (24h), the media was changed and cells cultured in drug free media for an additional 10-14 days. Cells were fixed, stained with crystal violet and colonies of > 50 cells / colony counted. Colony formation data were entered into the Calcusyn program and combination index (CI) values determined. A CI value of less than 1.00 indicates synergy. Treatment of CMV infected cells with GX reduced colony formation as a single agent by 0.63 +/- 0.02. Treatment of c-FLIP-s infected cells with GX reduced colony formation as a single agent by 0.72 +/- 0.01.

CMV + VEH				CMV + 50nM GX			
Sor (μM)	Val (mM)	Fa	CI	Sor (μM)	Val (mM)	Fa	CI
2.25	0.75	0.43	0.72	2.25	0.75	0.43	0.31
3.00	1.00	0.51	0.70	3.00	1.00	0.51	0.32
3.75	1.25	0.66	0.66	3.75	1.25	0.58	0.26
c-FLIP-s + VEH				**c-FLIP-s + 50nM GX**			
Sor (μM)	Val (mM)	Fa	CI	Sor (μM)	Val (mM)	Fa	CI
2.25	0.75	0.10	4.55	2.25	0.75	0.43	0.58
3.00	1.00	0.13	3.54	3.00	1.00	0.47	0.56
3.75	1.25	0.19	2.08	3.75	1.25	0.56	0.49

Figure 1A

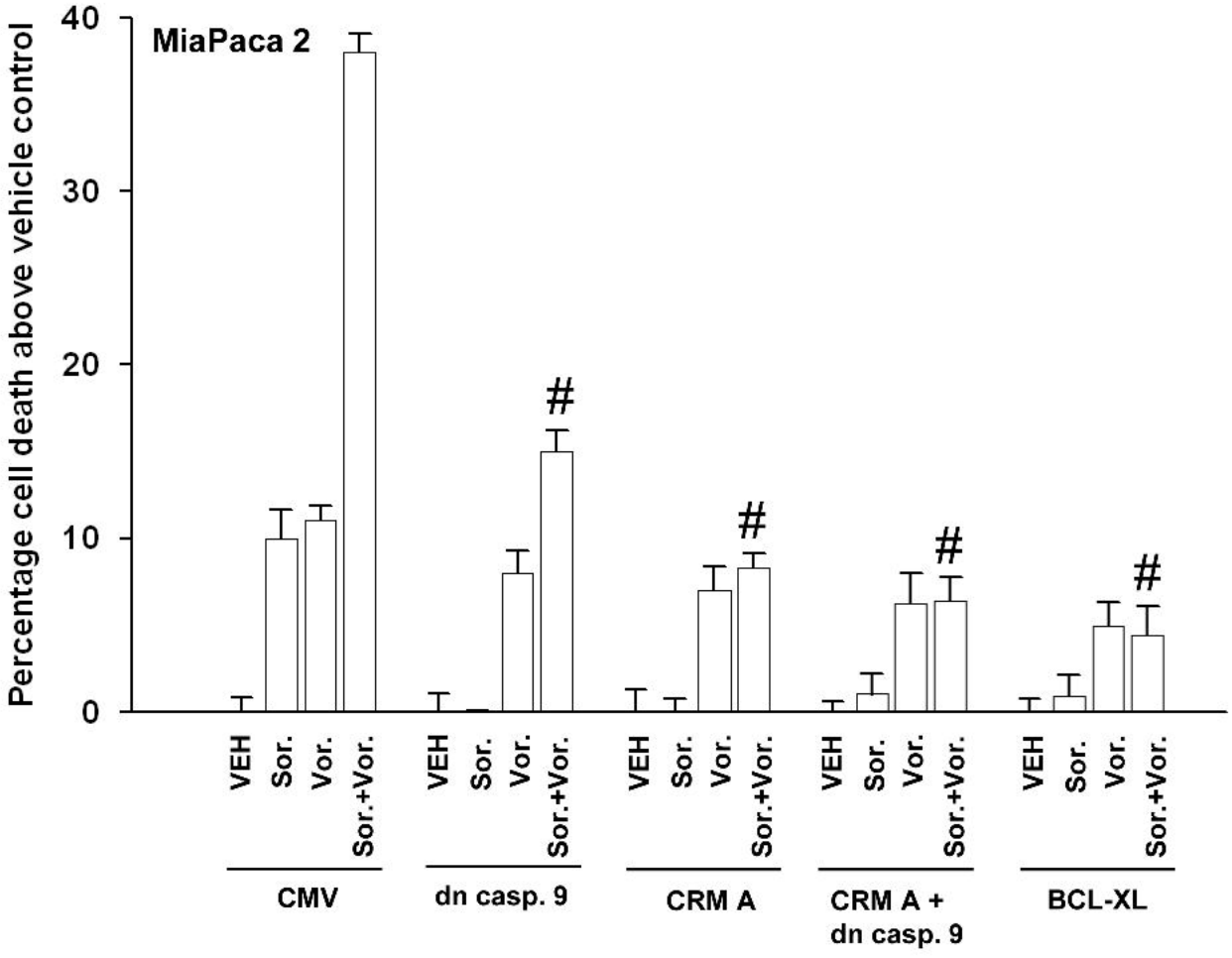
MiaPaca 2
Percentage cell death above vehicle control
40
30
20
10
0
#
#
#
#
VEH
Sor.
Vor.
Sor.+Vor.
CMV
dn casp. 9
CRM A
CRM A + dn casp. 9
BCL-XL

Figure 1B

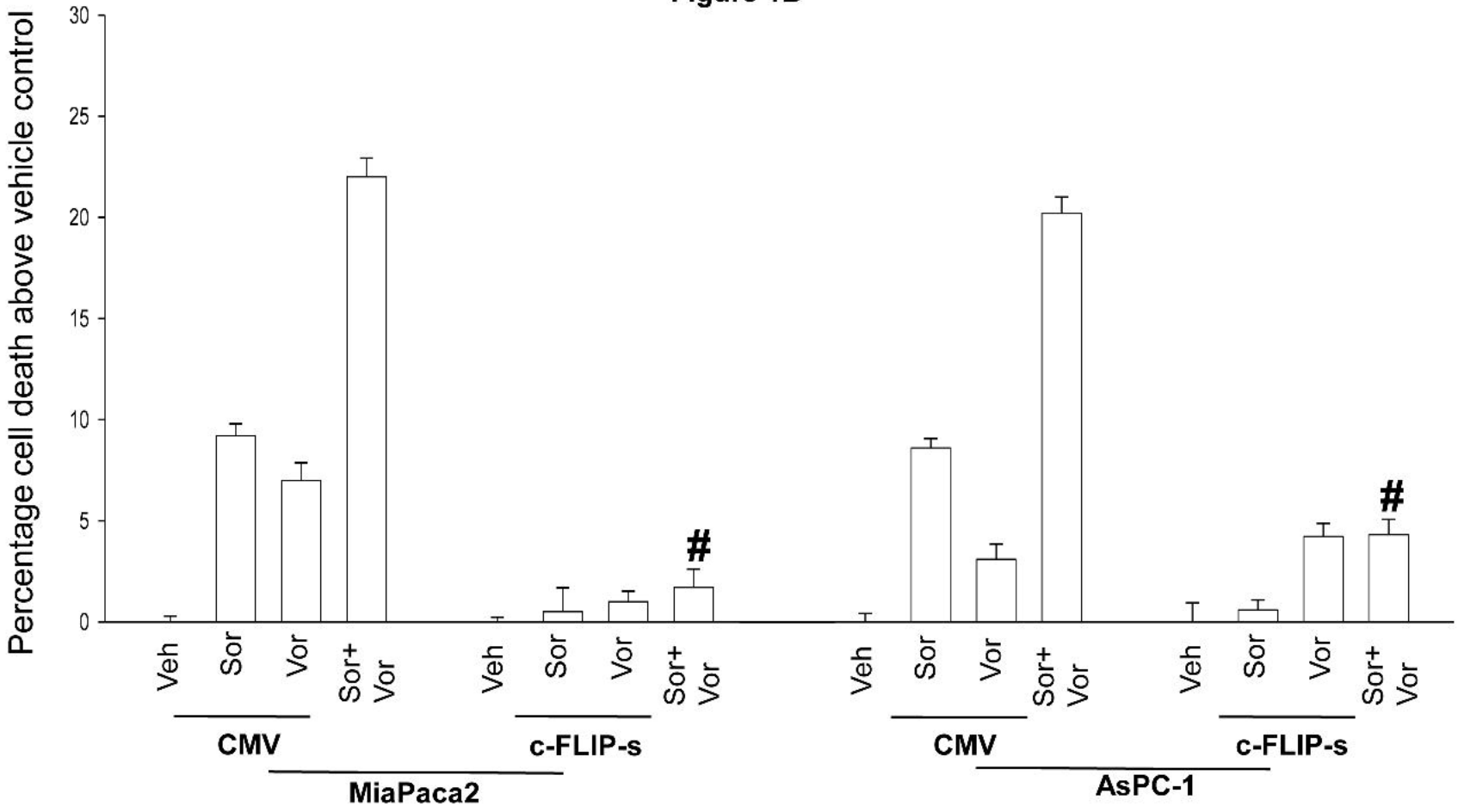
Percentage cell death above vehicle control
30
25
20
15
10
5
0
Veh
Sor
Vor
Sor+ Vor
Veh
Sor
Vor
Sor+ Vor
#
Veh
Sor
Vor
Sor+ Vor
Veh
Sor
Vor
Sor+ Vor
#
CMV
c-FLIP-s
MiaPaca2
CMV
c-FLIP-s
AsPC-1

Figure 1C

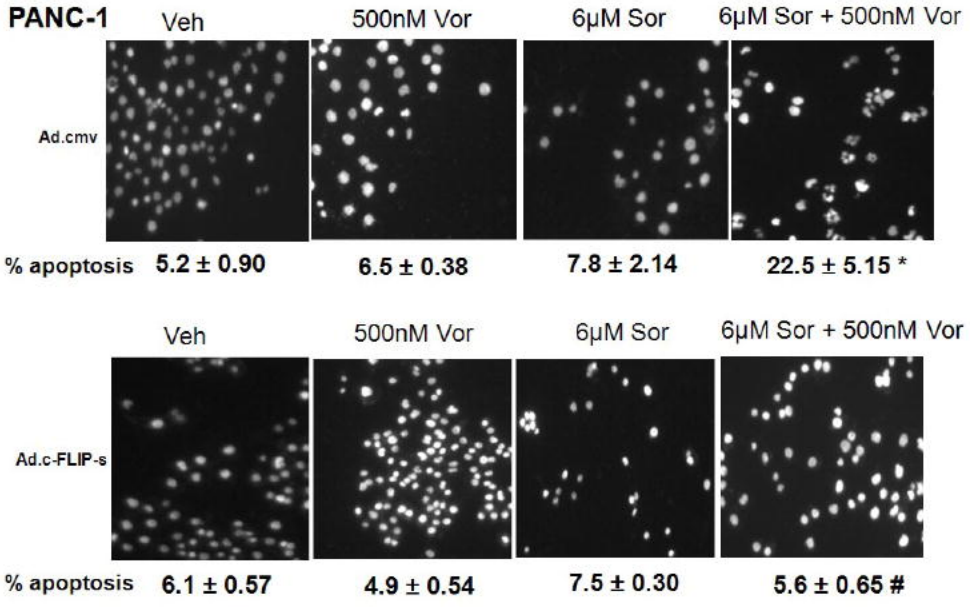
PANC-1
Veh
500nM Vor
6μM Sor
6μM Sor + 500nM Vor
Ad.cmv
% apoptosis
5.2 ± 0.90
6.5 ± 0.38
7.8 ± 2.14
22.5 ± 5.15 *
Veh
500nM Vor
6μM Sor
6μM Sor + 500nM Vor
Ad.c-FLIP-s
% apoptosis
6.1 ± 0.57
4.9 ± 0.54
7.5 ± 0.30
5.6 ± 0.65 #

Figure 1D

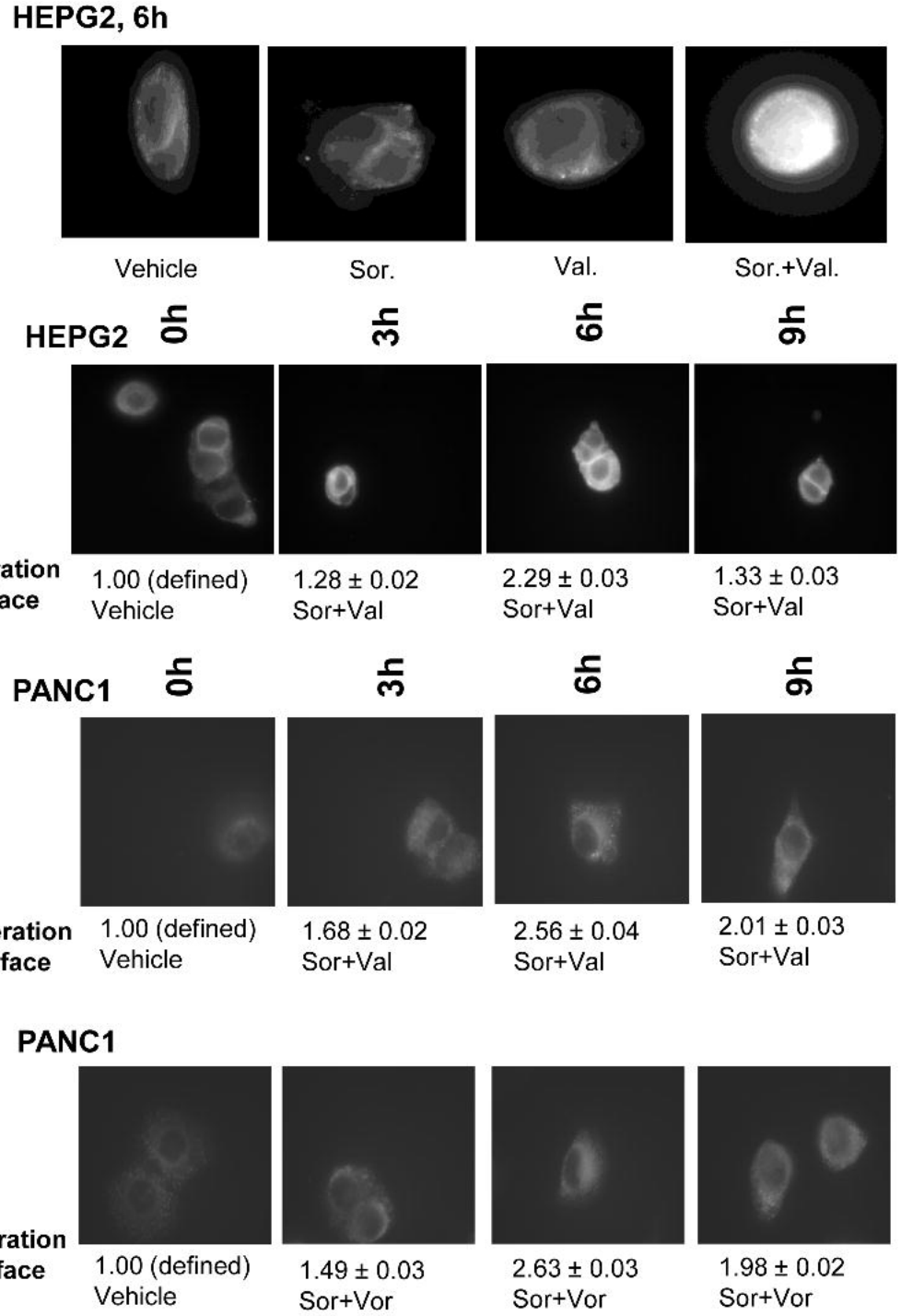
HEPG2, 6h
Vehicle
Sor.
Val.
Sor.+Val.
HEPG2
0h
3h
6h
9h
-Fold alteration CD95 surface intensity
1.00 (defined) Vehicle
1.28 ± 0.02 Sor+Val
2.29 ± 0.03 Sor+Val
1.33 ± 0.03 Sor+Val
PANC1
0h
3h
6h
9h
-Fold alteration CD95 surface intensity
1.00 (defined) Vehicle
1.68 ± 0.02 Sor+Val
2.56 ± 0.04 Sor+Val
2.01 ± 0.03 Sor+Val
PANC1
-Fold alteration CD95 surface intensity
1.00 (defined) Vehicle
1.49 ± 0.03 Sor+Vor
2.63 ± 0.03 Sor+Vor
1.98 ± 0.02 Sor+Vor

Figure 1E

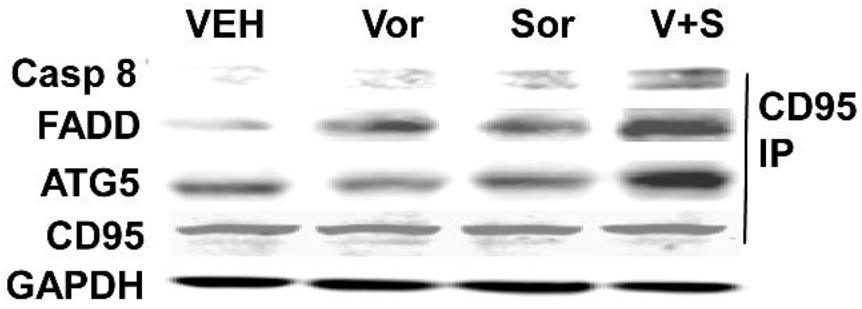

Figure 1F

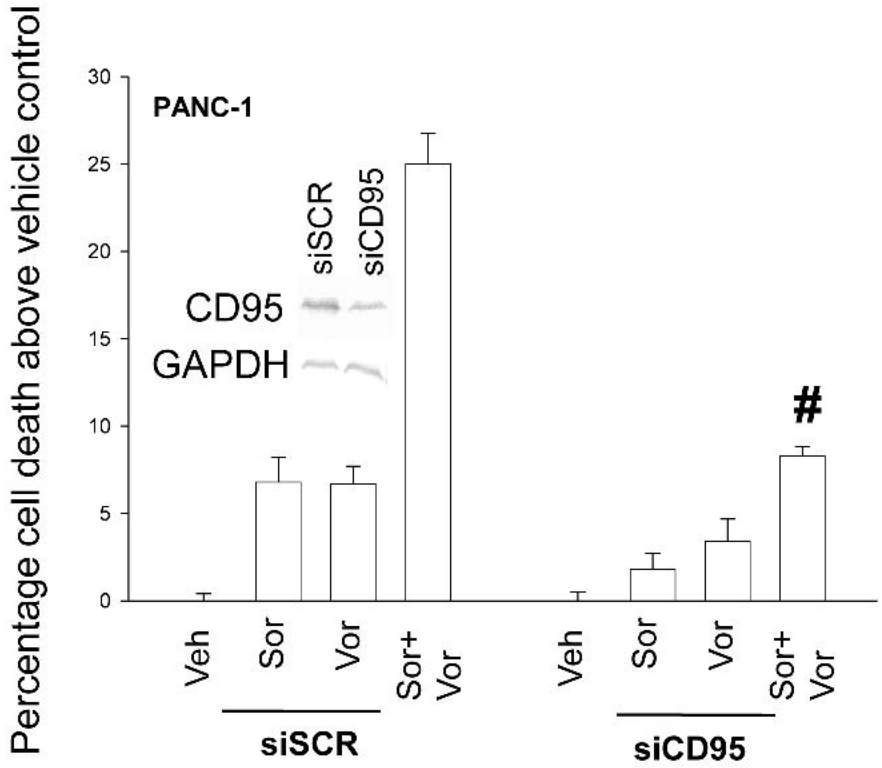
Percentage cell death above vehicle control
30
25
20
15
10
5
0
PANC-1
siSCR
siCD95
CD95
GAPDH
#
Veh
Sor
Vor
Sor+ Vor
Veh
Sor
Vor
Sor+ Vor
siSCR
siCD95

Figure 2A

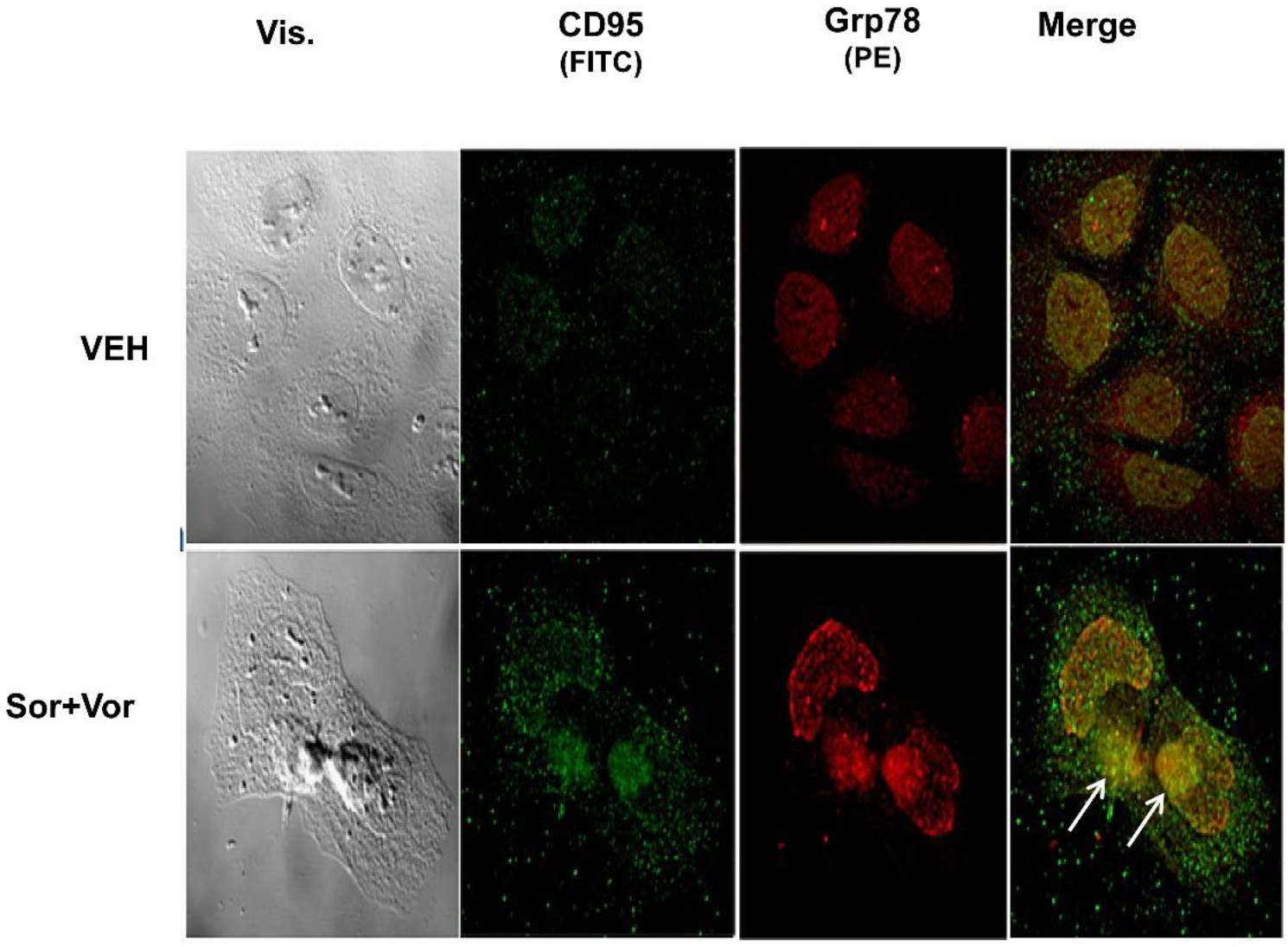

Figure 2B

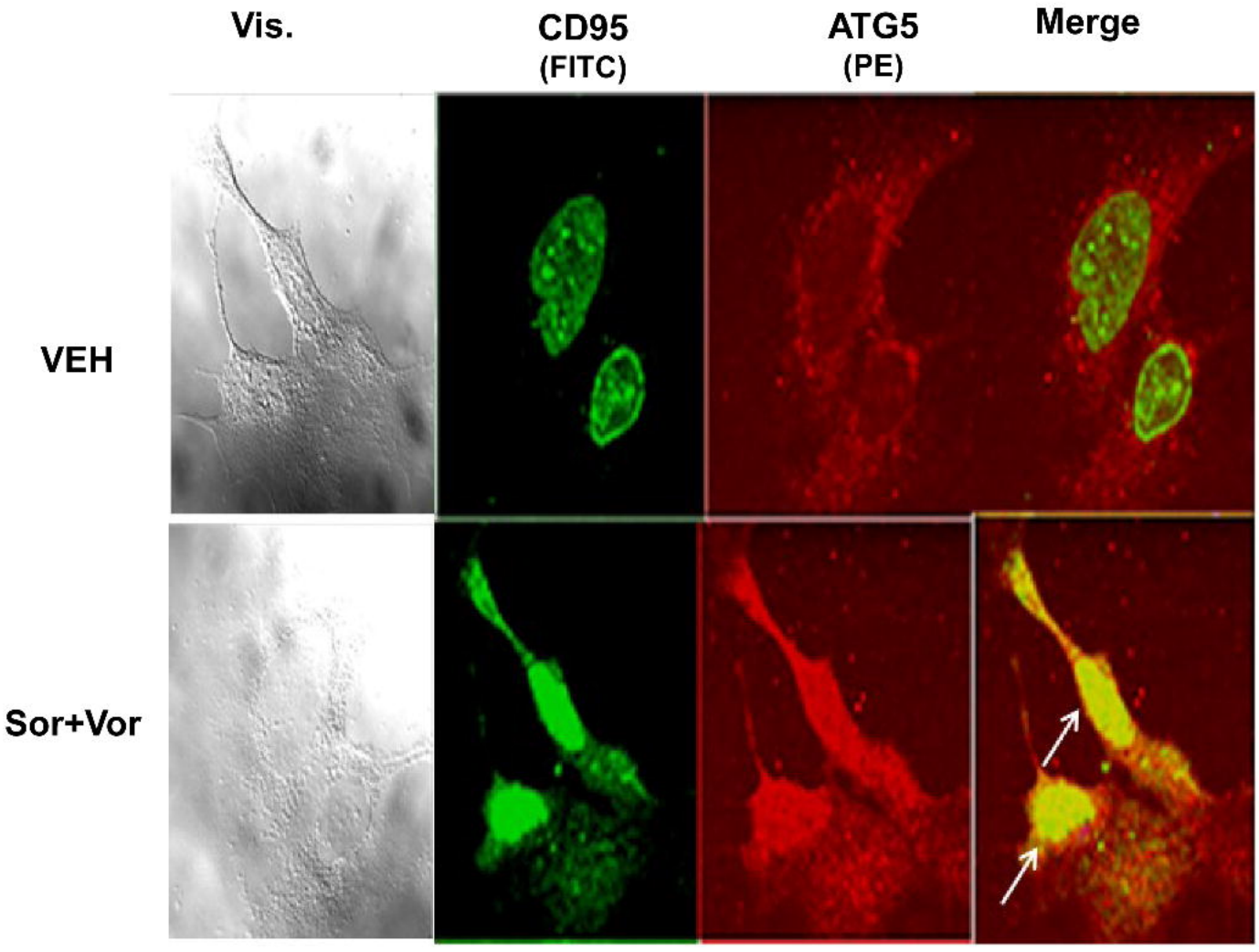

Figure 2C

HEP3B, 6h

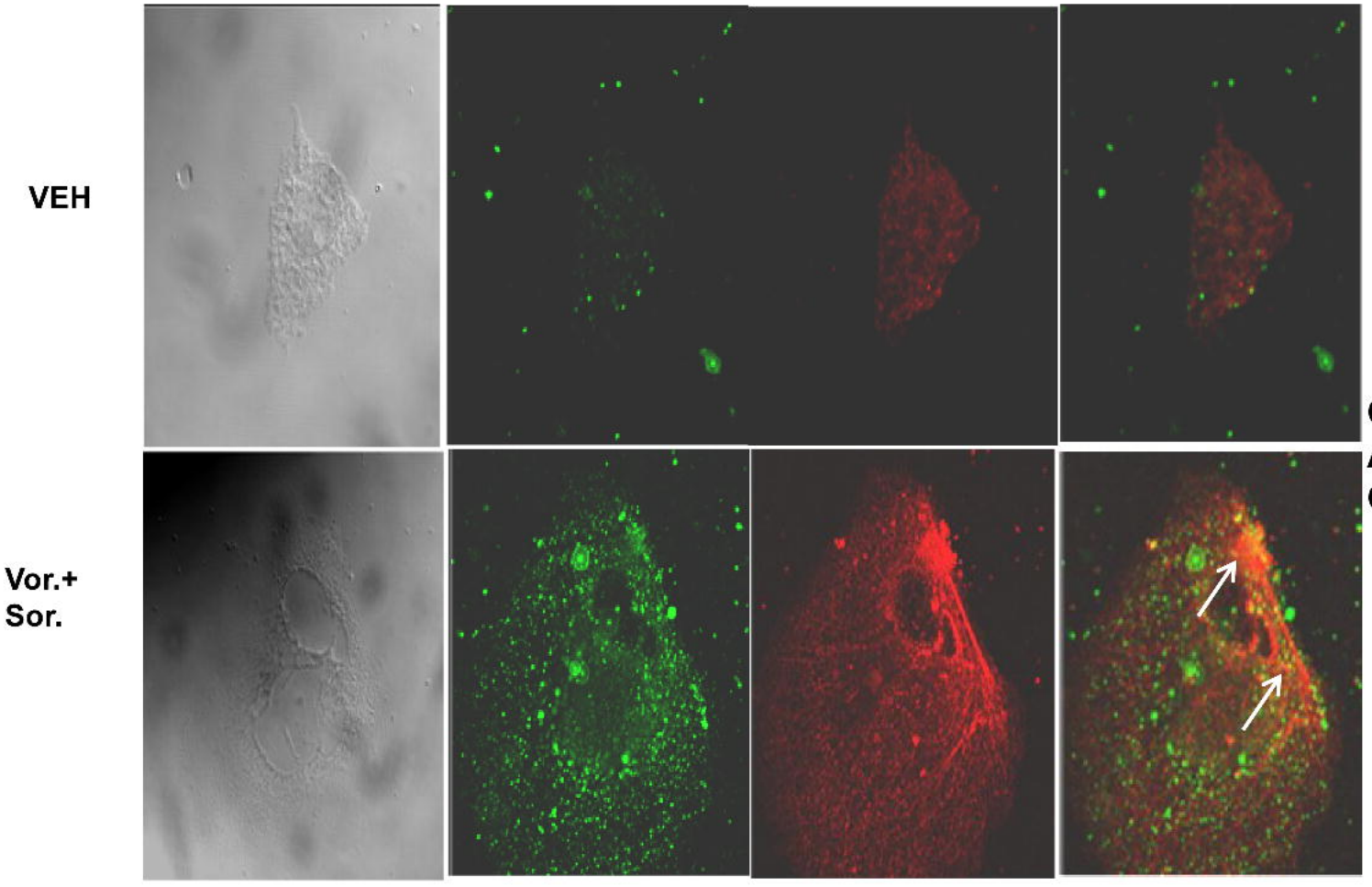

Figure 2D

HEP3B, 6h

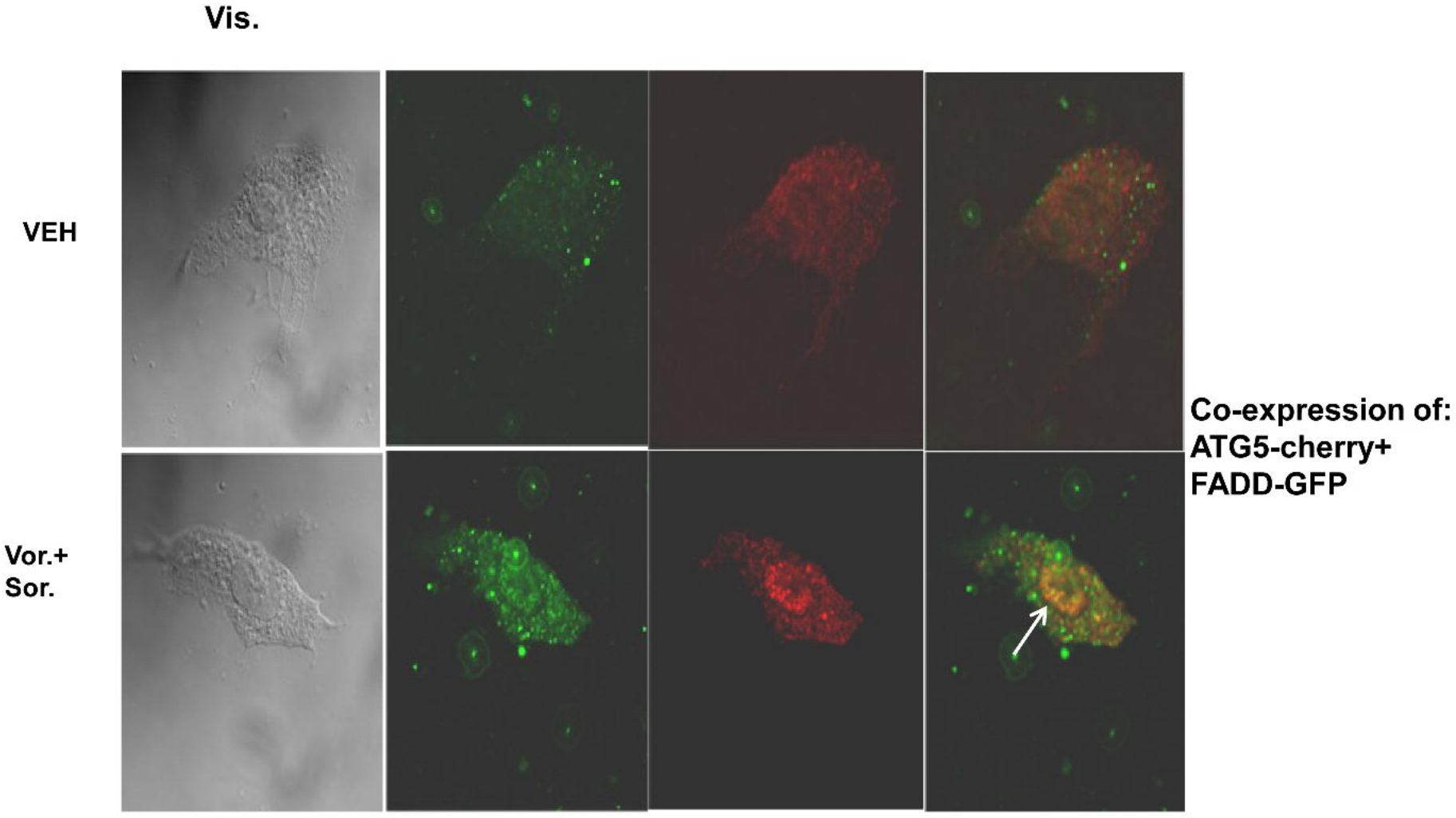

Figure 2E

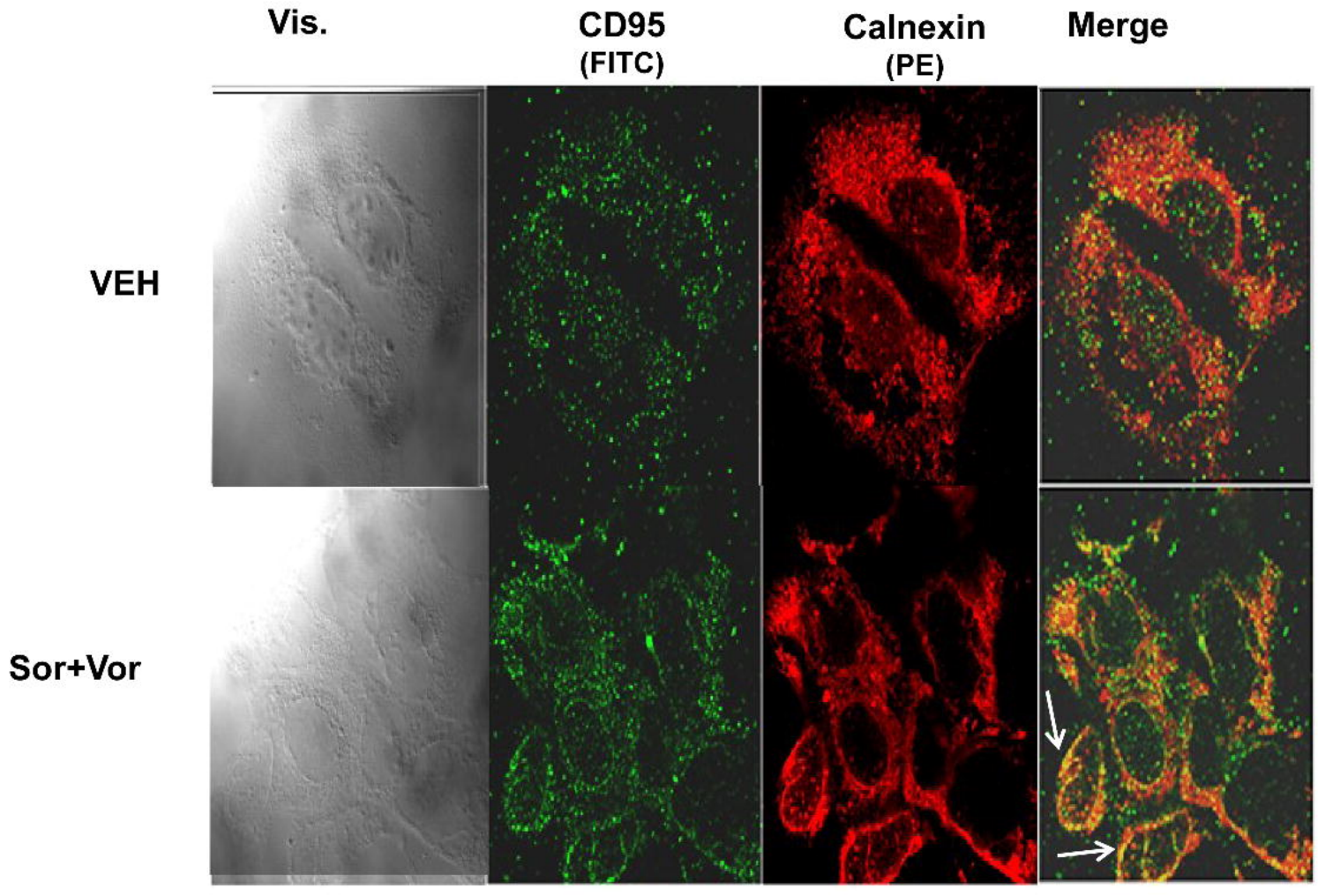

Figure 3A

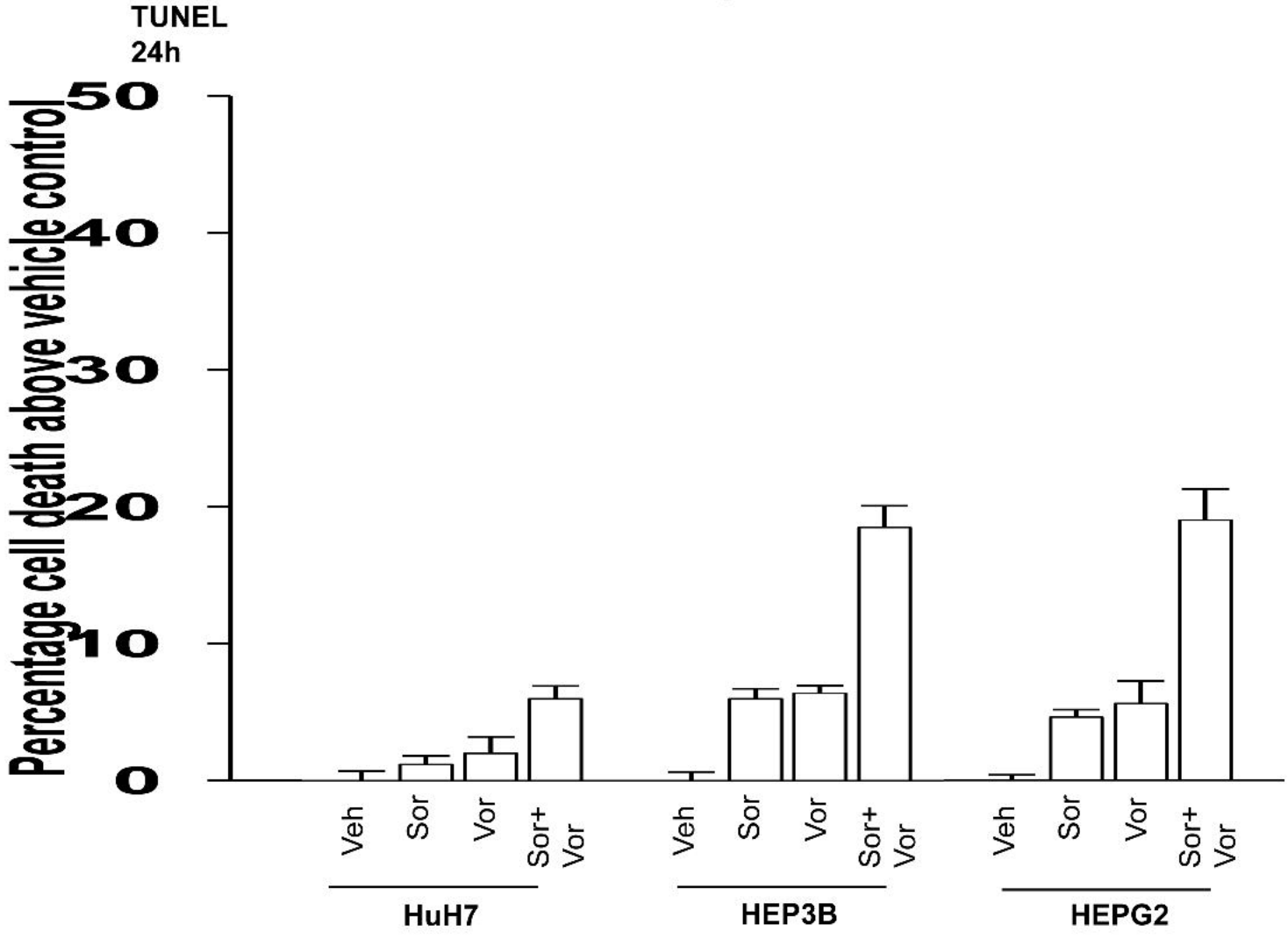
TUNEL
24h
Percentage cell death above vehicle control
0
10
20
30
40
50
Veh
Sor
Vor
Sor+ Vor
HuH7
HEP3B
HEPG2

Figure 3B

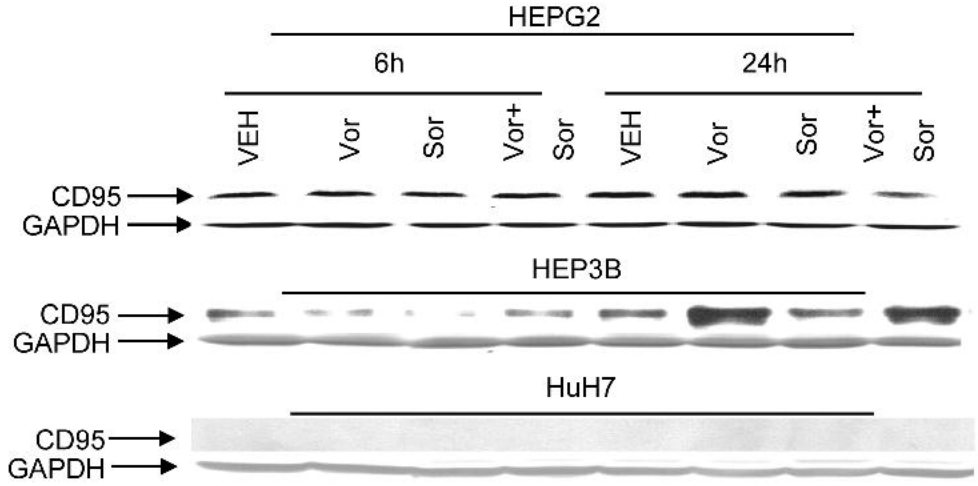
HEPG2
6h
24h
VEH
Vor
Sor
Vor+
Sor
VEH
Vor
Sor
Vor+
Sor
CD95
GAPDH
HEP3B
CD95
GAPDH
HuH7
CD95
GAPDH

Figure 3C

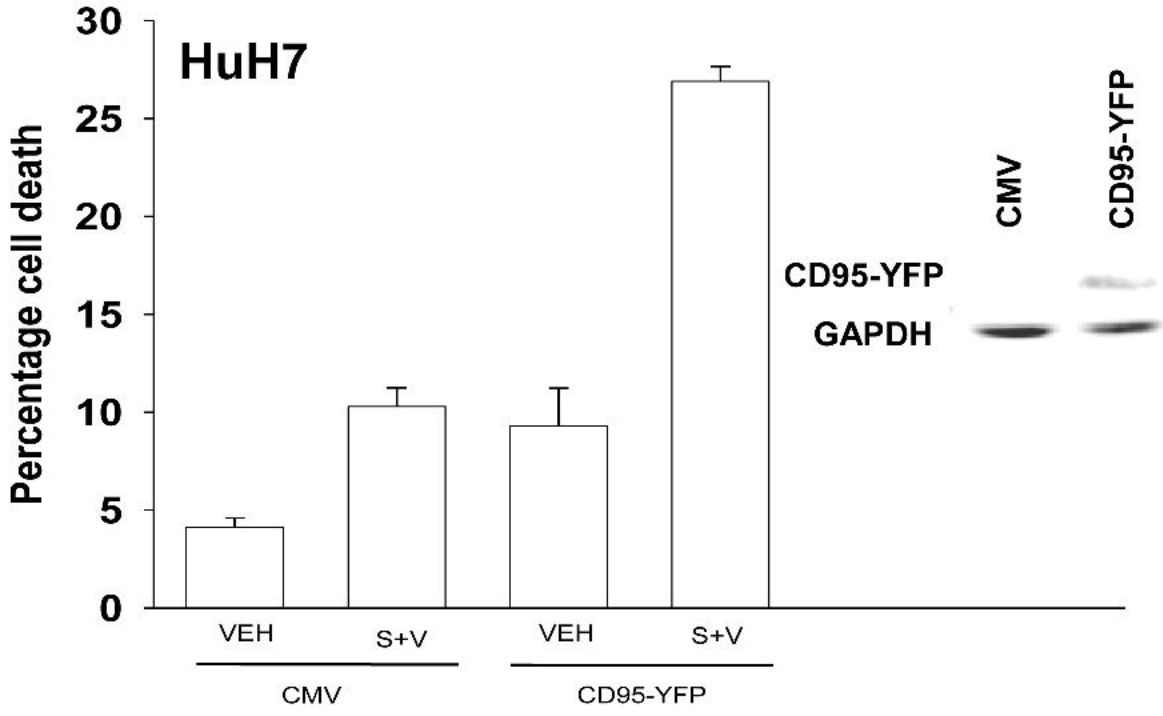
HuH7
Percentage cell death
30
25
20
15
10
5
0
VEH
S+V
VEH
S+V
CMV
CD95-YFP
CMV
CD95-YFP
CD95-YFP
GAPDH

Figure 3D

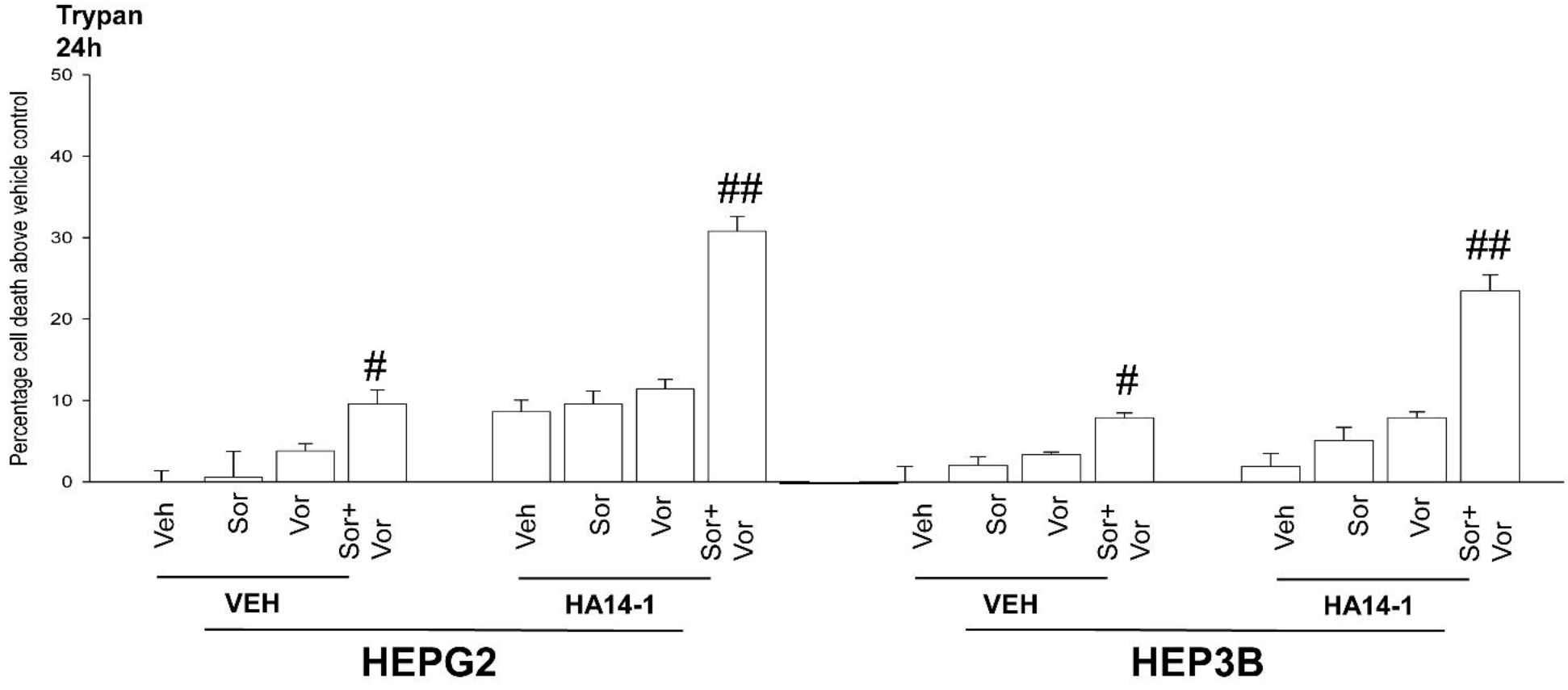
Trypan
24h
Percentage cell death above vehicle control
50
40
30
20
10
0
#
##
#
##
Veh
Sor
Vor
Sor+ Vor
VEH
HA14-1
HEPG2
HEP3B

Figure 3E

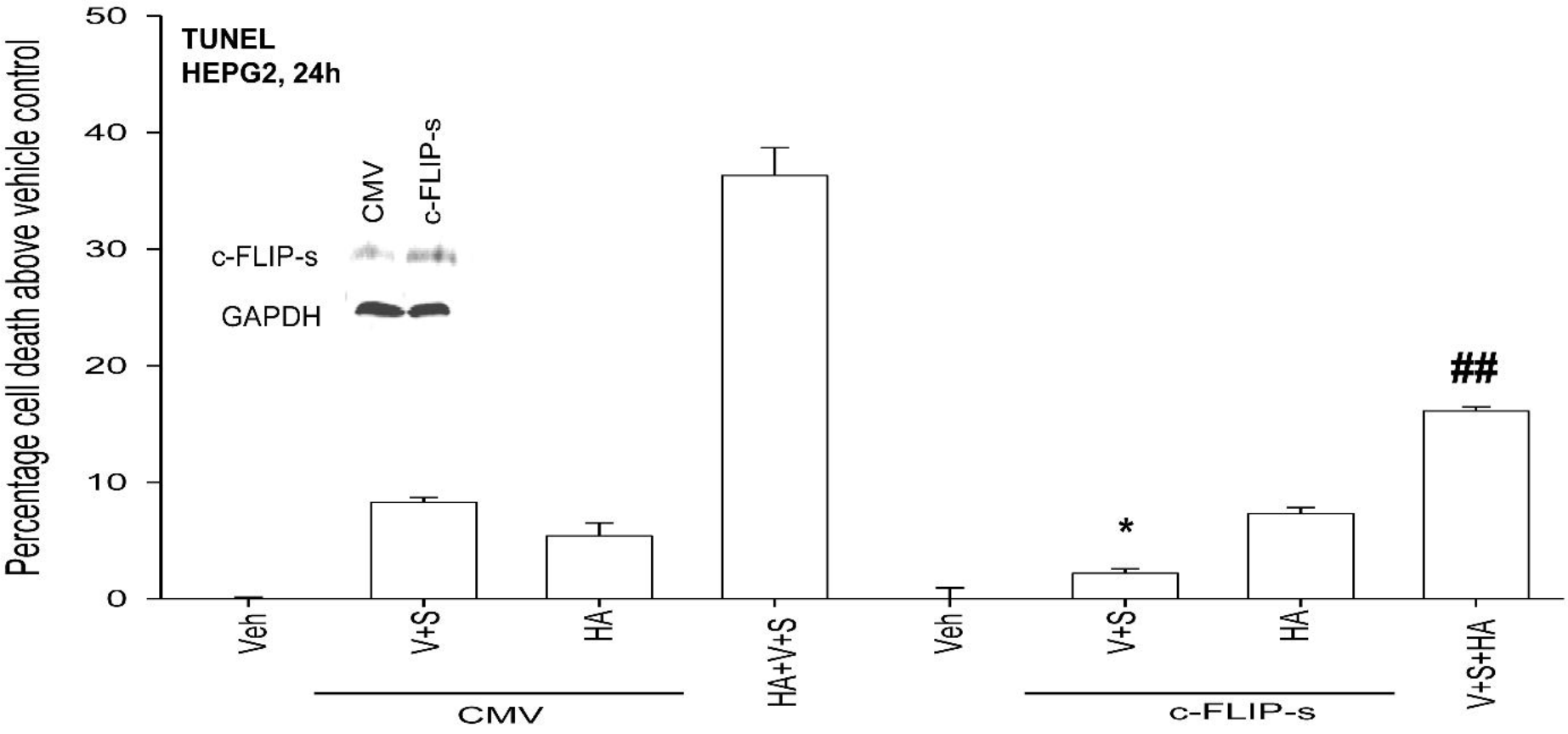
TUNEL
HEPG2, 24h
Percentage cell death above vehicle control
50
40
30
20
10
0
CMV
c-FLIP-s
c-FLIP-s
GAPDH
*
##
Veh
V+S
HA
HA+V+S
Veh
V+S
HA
V+S+HA
CMV
c-FLIP-s

Figure 3F

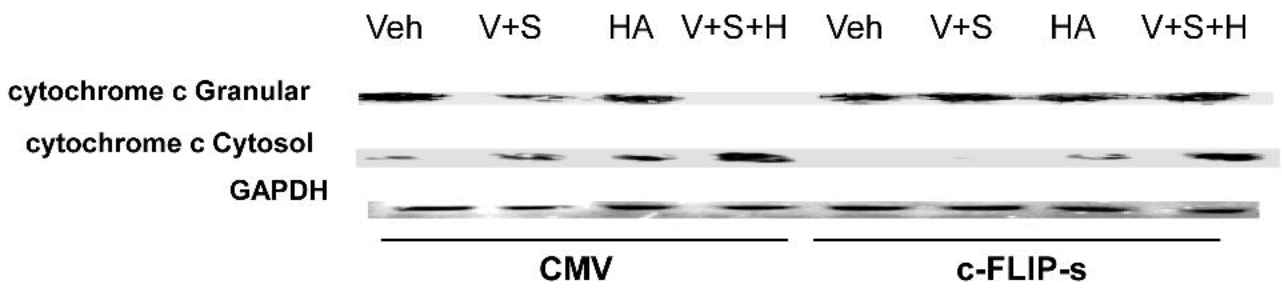
Veh
V+S
HA
V+S+H
Veh
V+S
HA
V+S+H
cytochrome c Granular
cytochrome c Cytosol
GAPDH
CMV
c-FLIP-s

Figure 3G

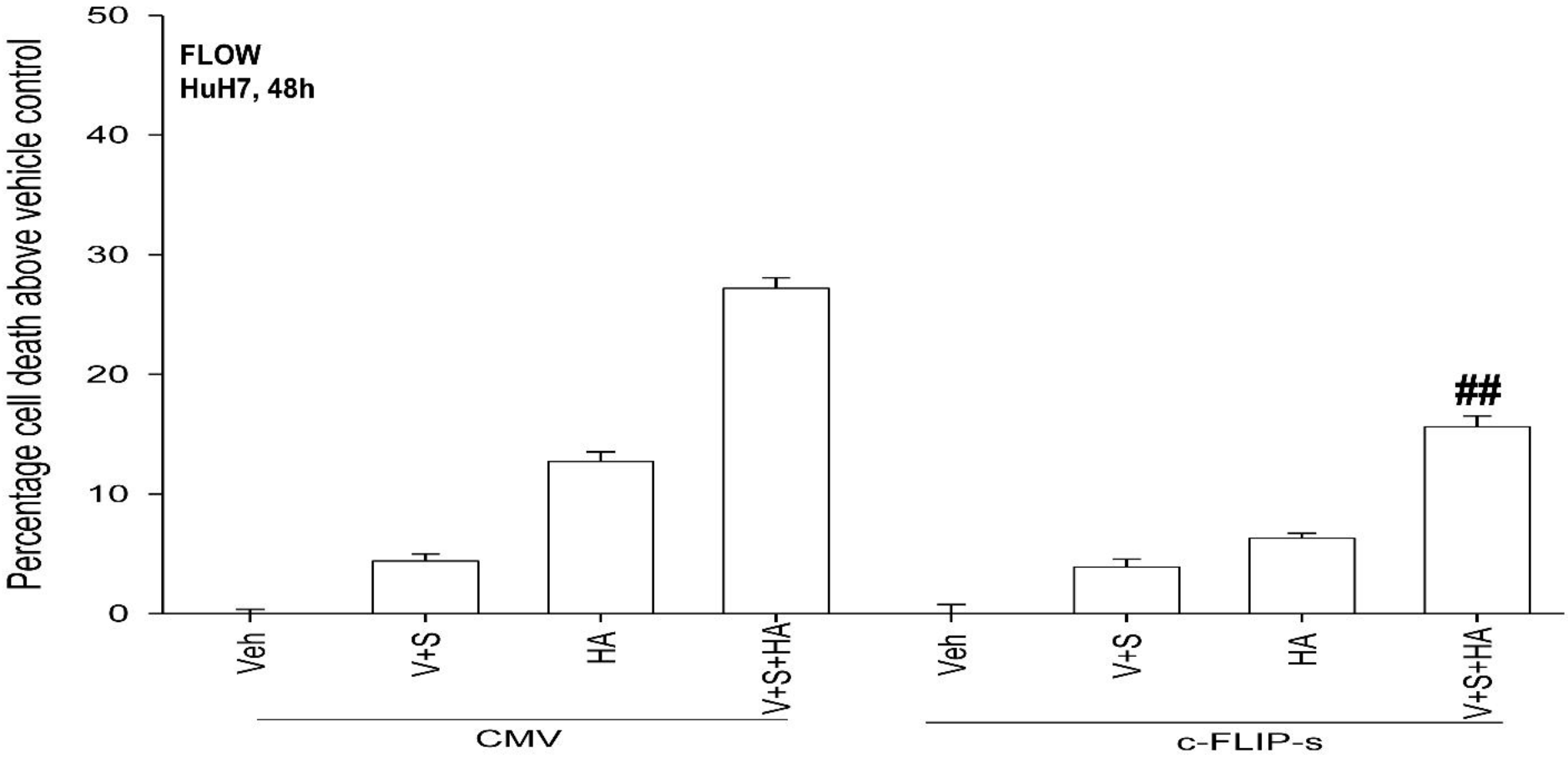
FLOW
HuH7, 48h
Percentage cell death above vehicle control
50
40
30
20
10
0
##
Veh
V+S
HA
V+S+HA
Veh
V+S
HA
V+S+HA
CMV
c-FLIP-s

Figure 3H

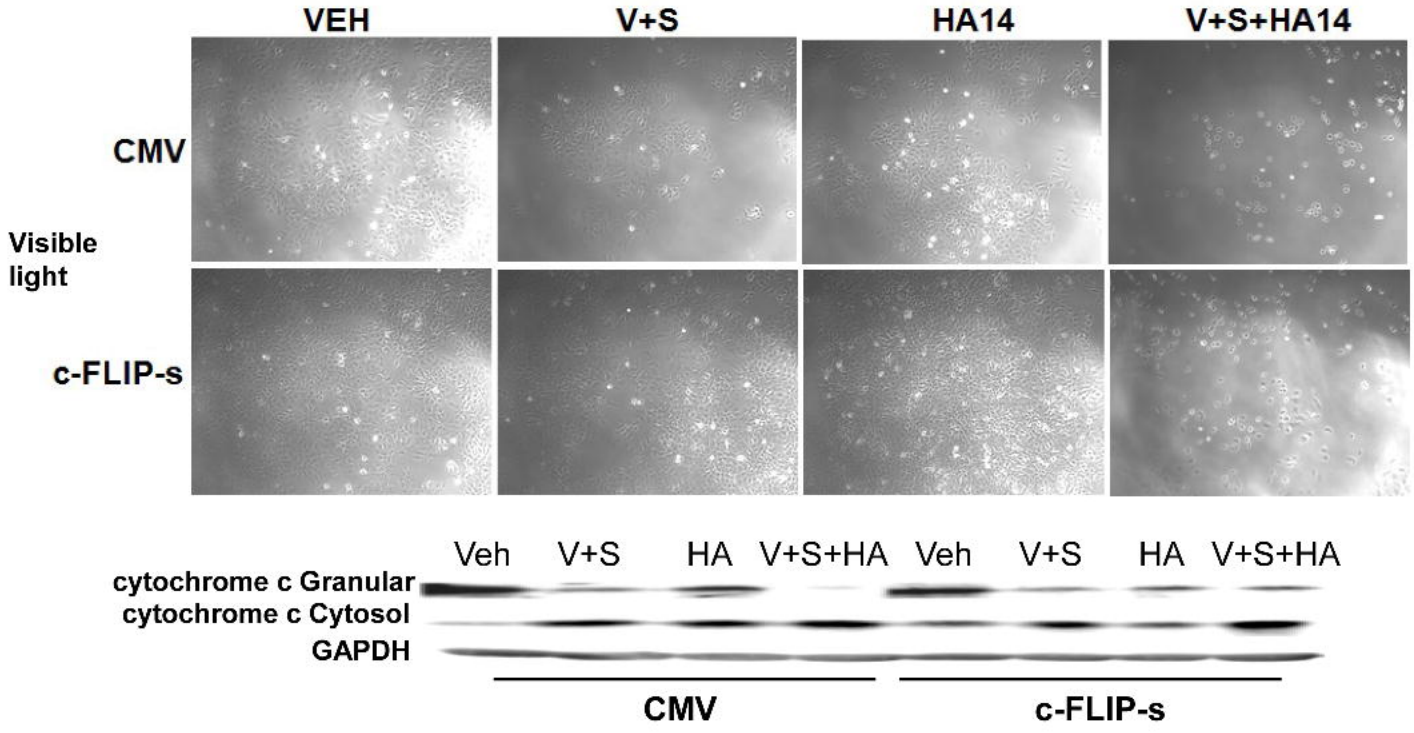
VEH
V+S
HA14
V+S+HA14
CMV
Visible light
c-FLIP-s
Veh
V+S
HA
V+S+HA
Veh
V+S
HA
V+S+HA
cytochrome c Granular
cytochrome c Cytosol
GAPDH
CMV
c-FLIP-s

Figure 4A

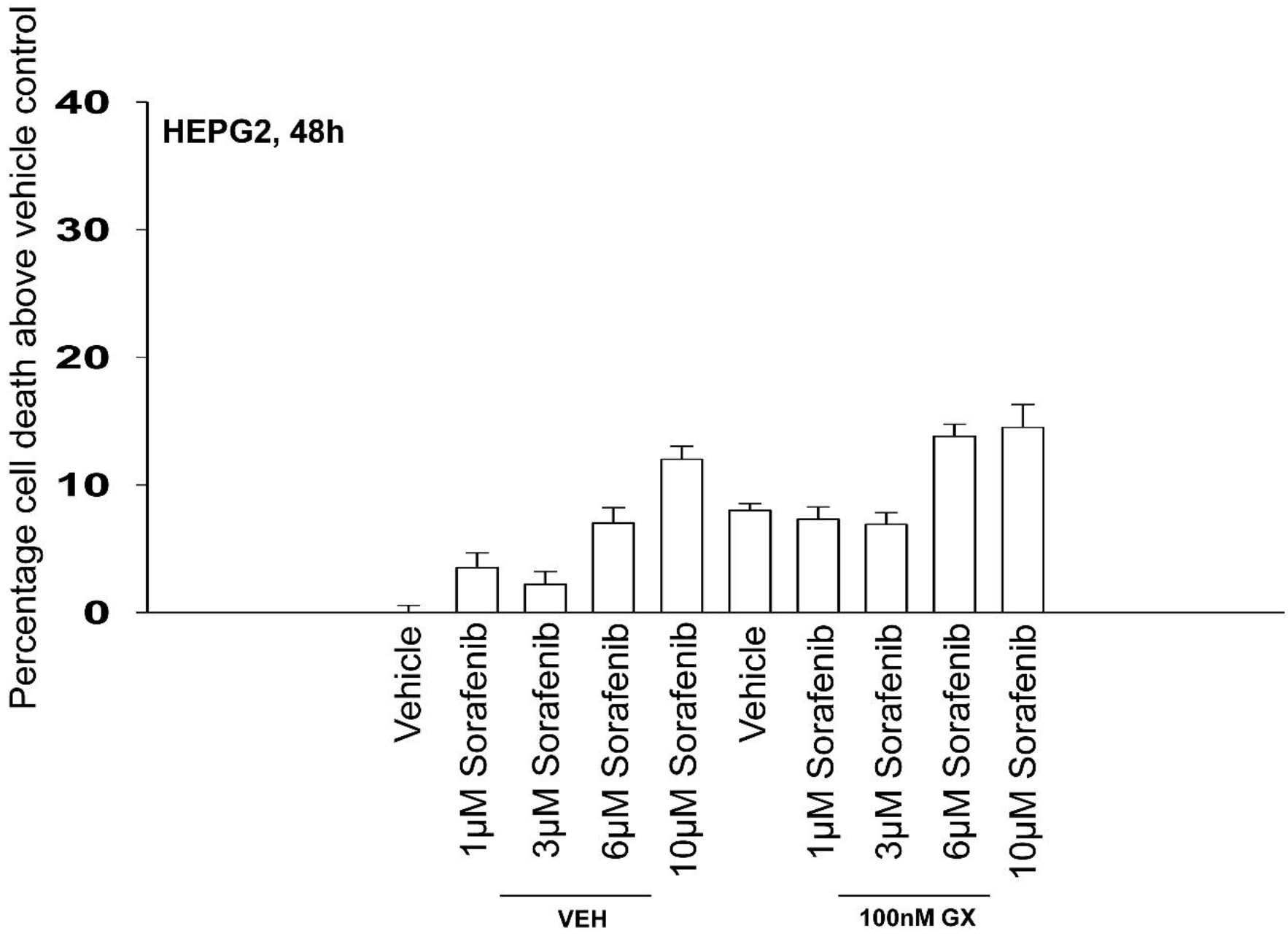
Percentage cell death above vehicle control
40
30
20
10
0
HEPG2, 48h
Vehicle
1μM Sorafenib
3μM Sorafenib
6μM Sorafenib
10μM Sorafenib
Vehicle
1μM Sorafenib
3μM Sorafenib
6μM Sorafenib
10μM Sorafenib
VEH
100nM GX

Figure 4B

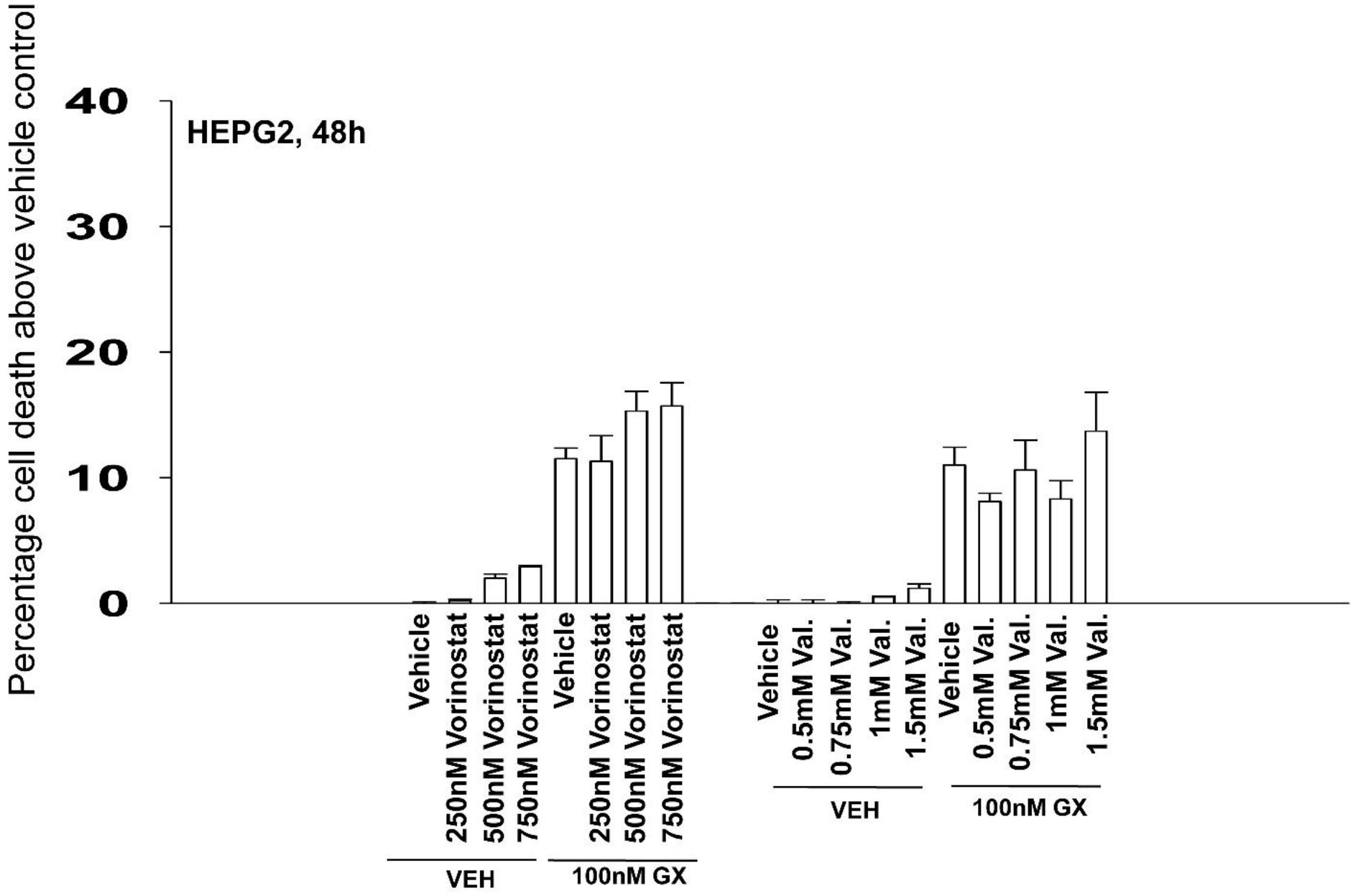
Percentage cell death above vehicle control
40
30
20
10
0
HEPG2, 48h
Vehicle
250nM Vorinostat
500nM Vorinostat
750nM Vorinostat
Vehicle
250nM Vorinostat
500nM Vorinostat
750nM Vorinostat
VEH
100nM GX
Vehicle
0.5mM Val.
0.75mM Val.
1mM Val.
1.5mM Val.
Vehicle
0.5mM Val.
0.75mM Val.
1mM Val.
1.5mM Val.
VEH
100nM GX

Figure 4C

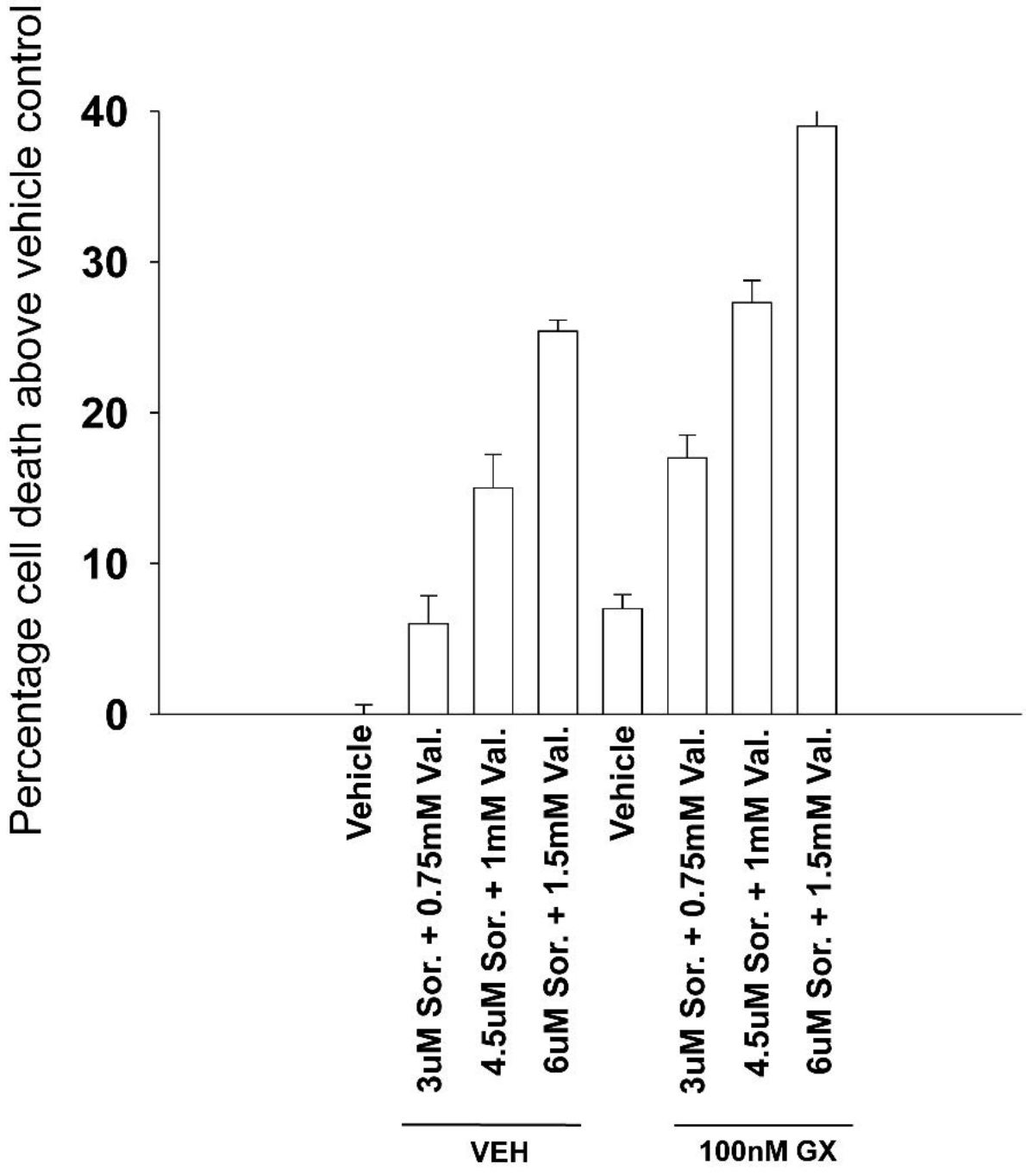
Percentage cell death above vehicle control
0
10
20
30
40
Vehicle
3uM Sor. + 0.75mM Val.
4.5uM Sor. + 1mM Val.
6uM Sor. + 1.5mM Val.
Vehicle
3uM Sor. + 0.75mM Val.
4.5uM Sor. + 1mM Val.
6uM Sor. + 1.5mM Val.
VEH
100nM GX

Figure 4D

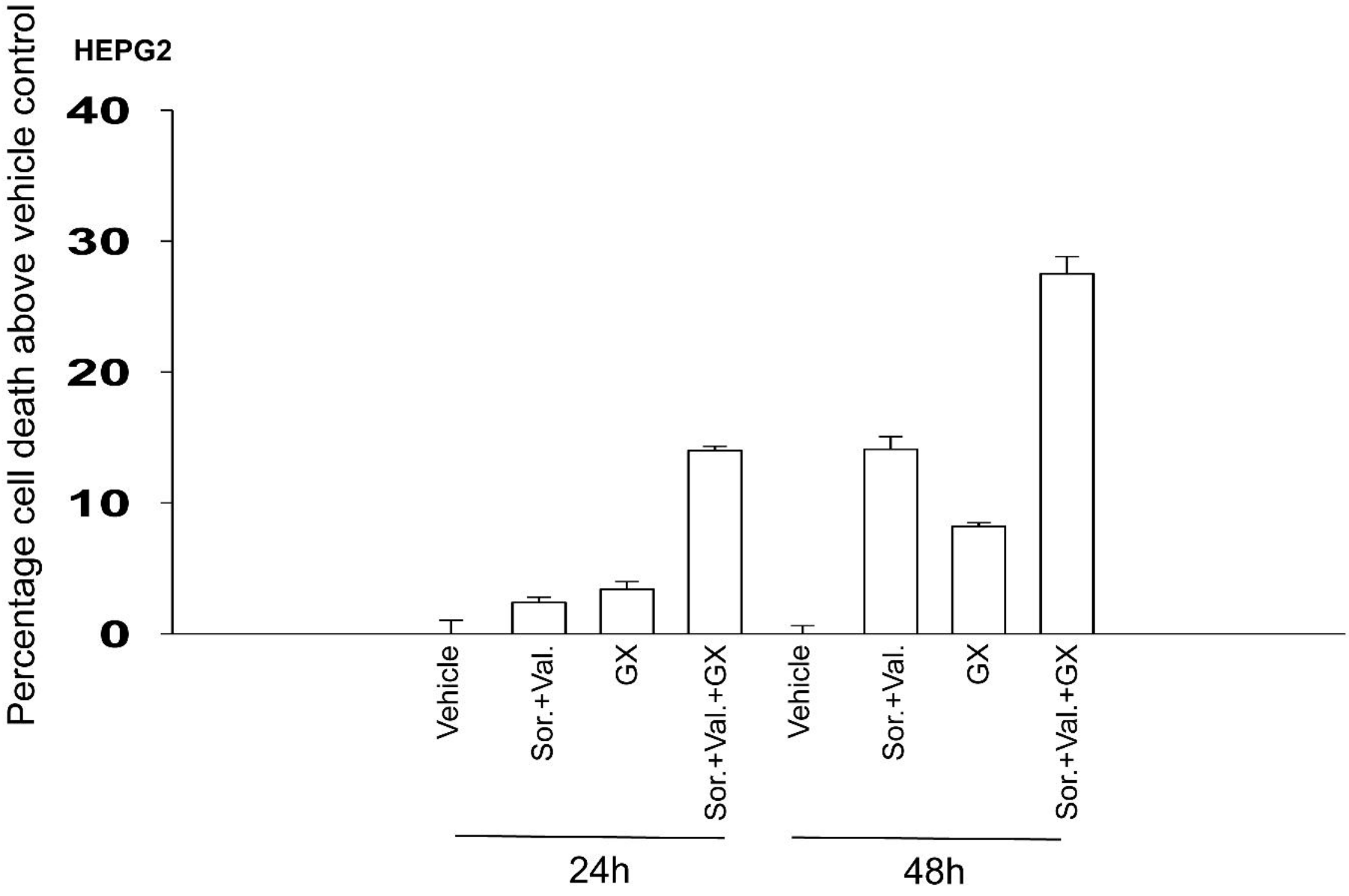
HEPG2
Percentage cell death above vehicle control
40
30
20
10
0
Vehicle
Sor.+Val.
GX
Sor.+Val.+GX
Vehicle
Sor.+Val.
GX
Sor.+Val.+GX
24h
48h

Figure 4E

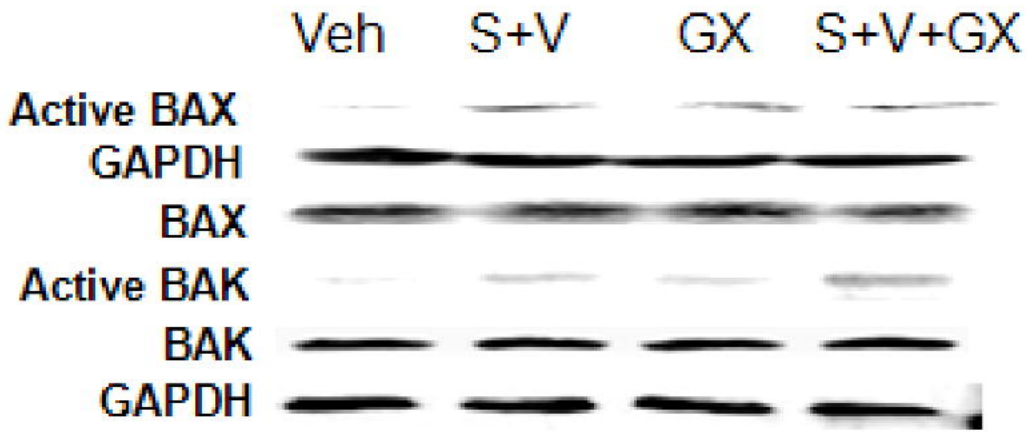

Figure 4F

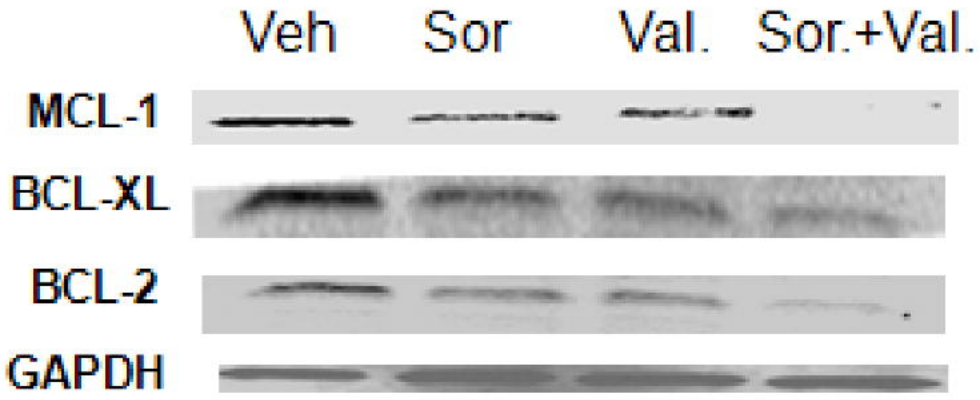

Figure 5A

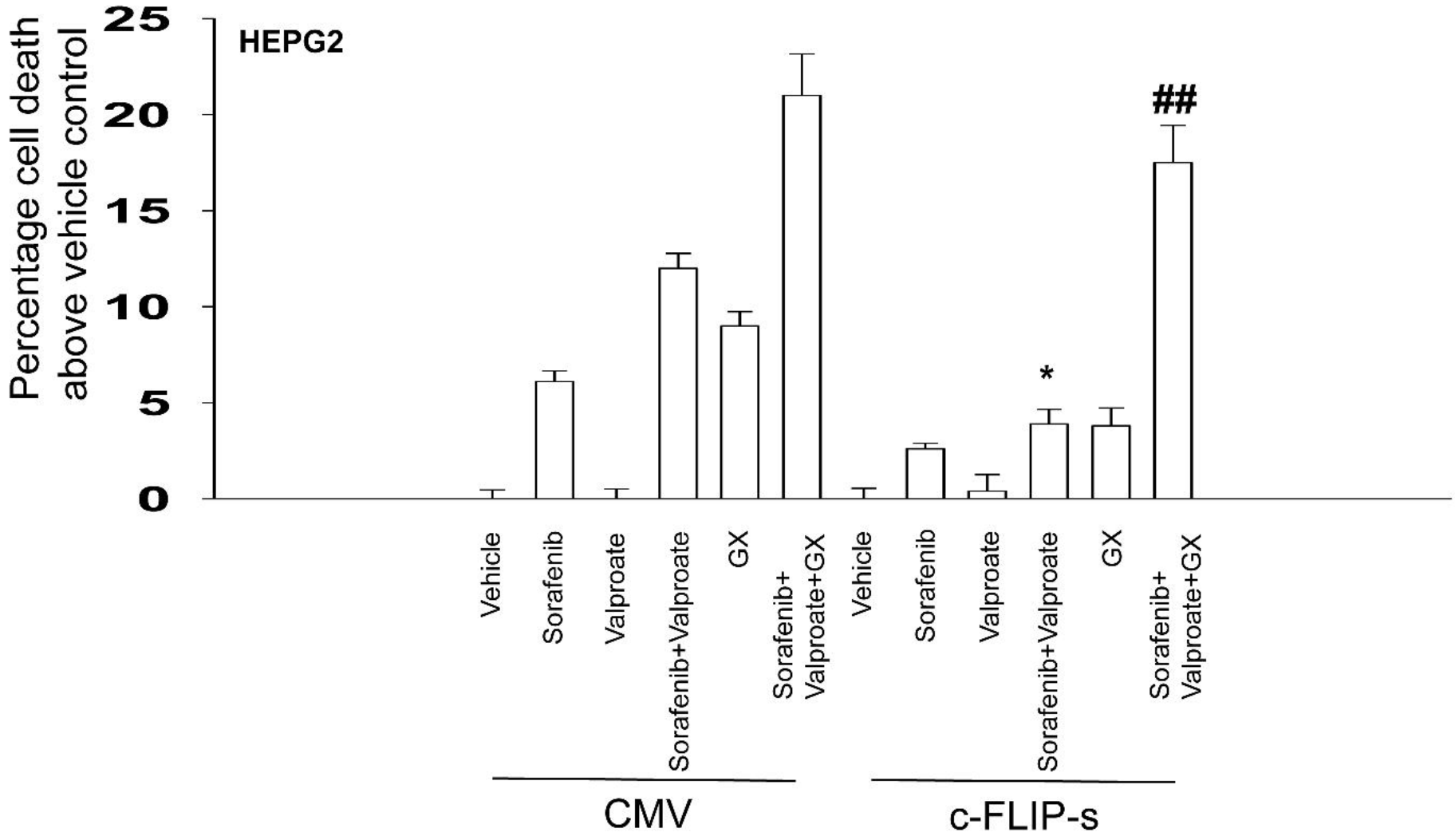
HEPG2
Percentage cell death above vehicle control
25
20
15
10
5
0
##
*
Vehicle
Sorafenib
Valproate
Sorafenib+Valproate
GX
Sorafenib+ Valproate+GX
Vehicle
Sorafenib
Valproate
Sorafenib+Valproate
GX
Sorafenib+ Valproate+GX
CMV
c-FLIP-s

Figure 5B

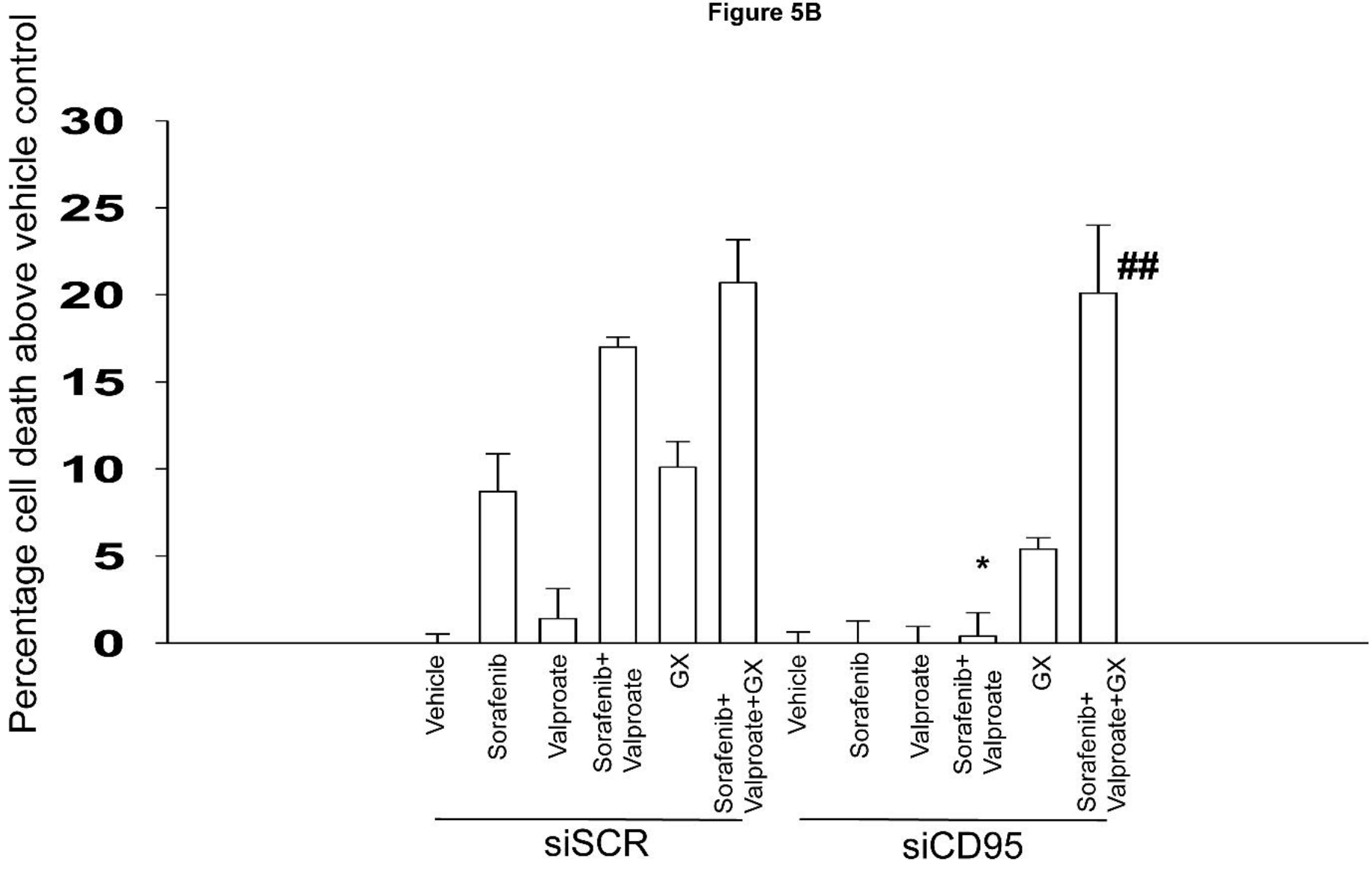
Percentage cell death above vehicle control
30
25
20
15
10
5
0
##
*
Vehicle
Sorafenib
Valproate
Sorafenib+ Valproate
GX
Sorafenib+ Valproate+GX
Vehicle
Sorafenib
Valproate
Sorafenib+ Valproate
GX
Sorafenib+ Valproate+GX
siSCR
siCD95

Figure 5C

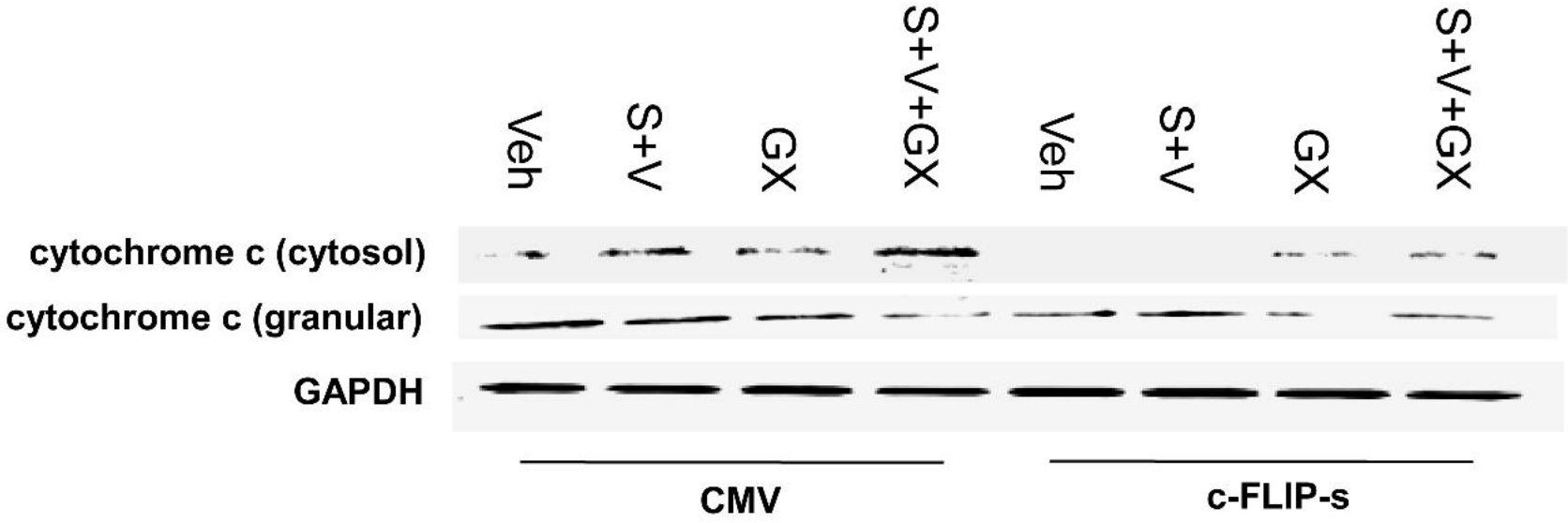
Veh
S+V
GX
S+V+GX
Veh
S+V
GX
S+V+GX
cytochrome c (cytosol)
cytochrome c (granular)
GAPDH
CMV
c-FLIP-s

Figure 5D

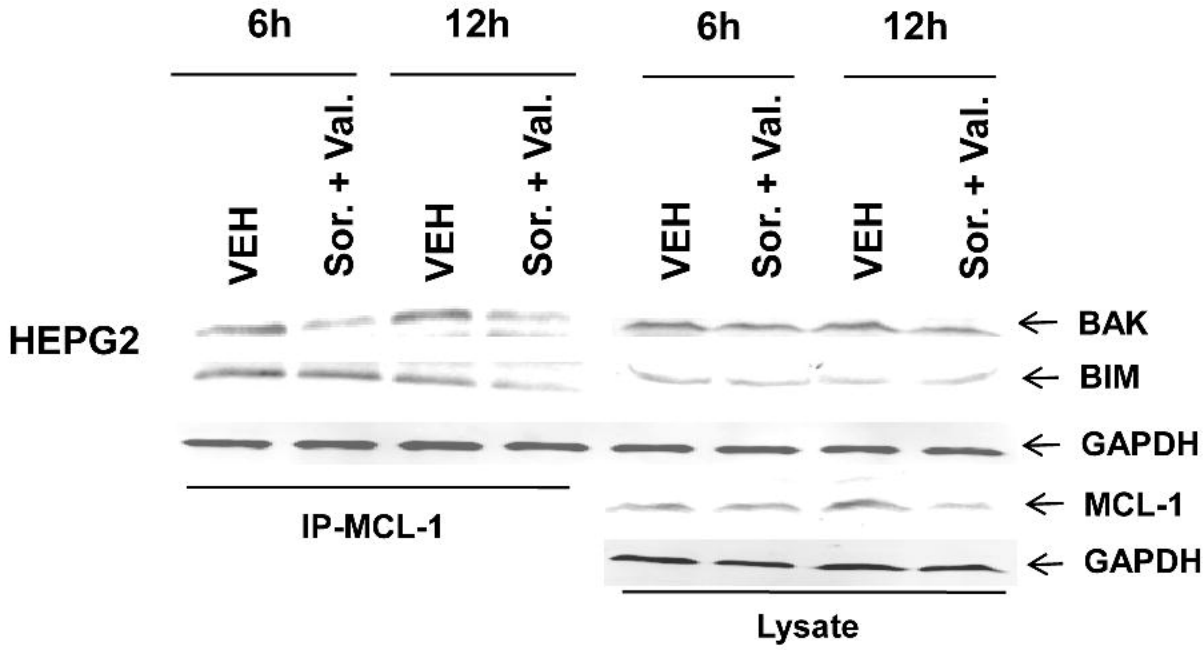
6h
12h
6h
12h
VEH
Sor. + Val.
VEH
Sor. + Val.
VEH
Sor. + Val.
VEH
Sor. + Val.
HEPG2
BAK
BIM
GAPDH
MCL-1
GAPDH
IP-MCL-1
Lysate

Figure 5E

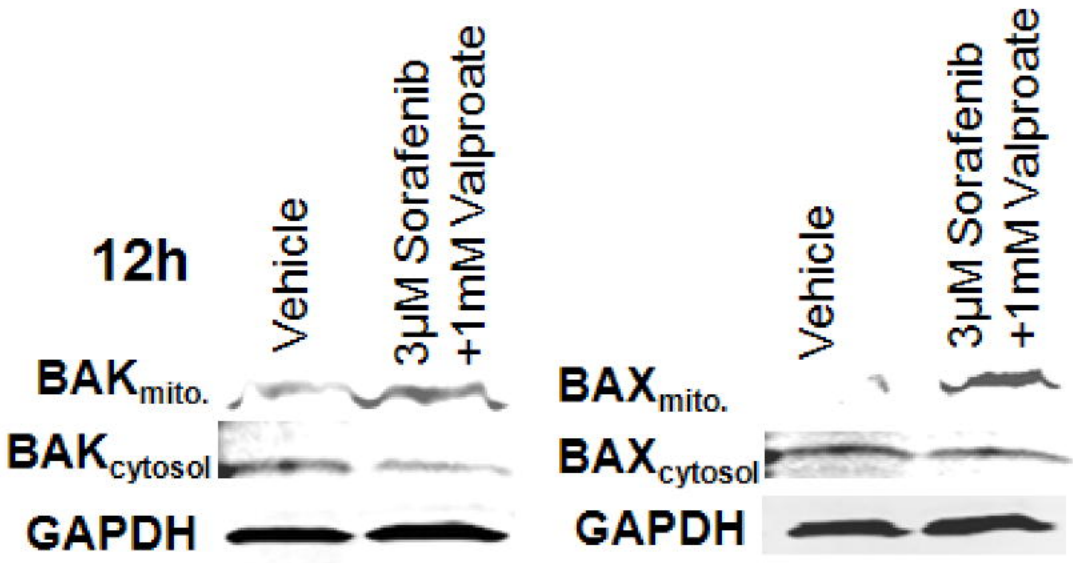
12h
Vehicle
3μM Sorafenib
+1mM Valproate
BAK mito.
BAK cytosol
GAPDH
Vehicle
3μM Sorafenib
+1mM Valproate
BAX mito.
BAX cytosol
GAPDH

Figure 6A

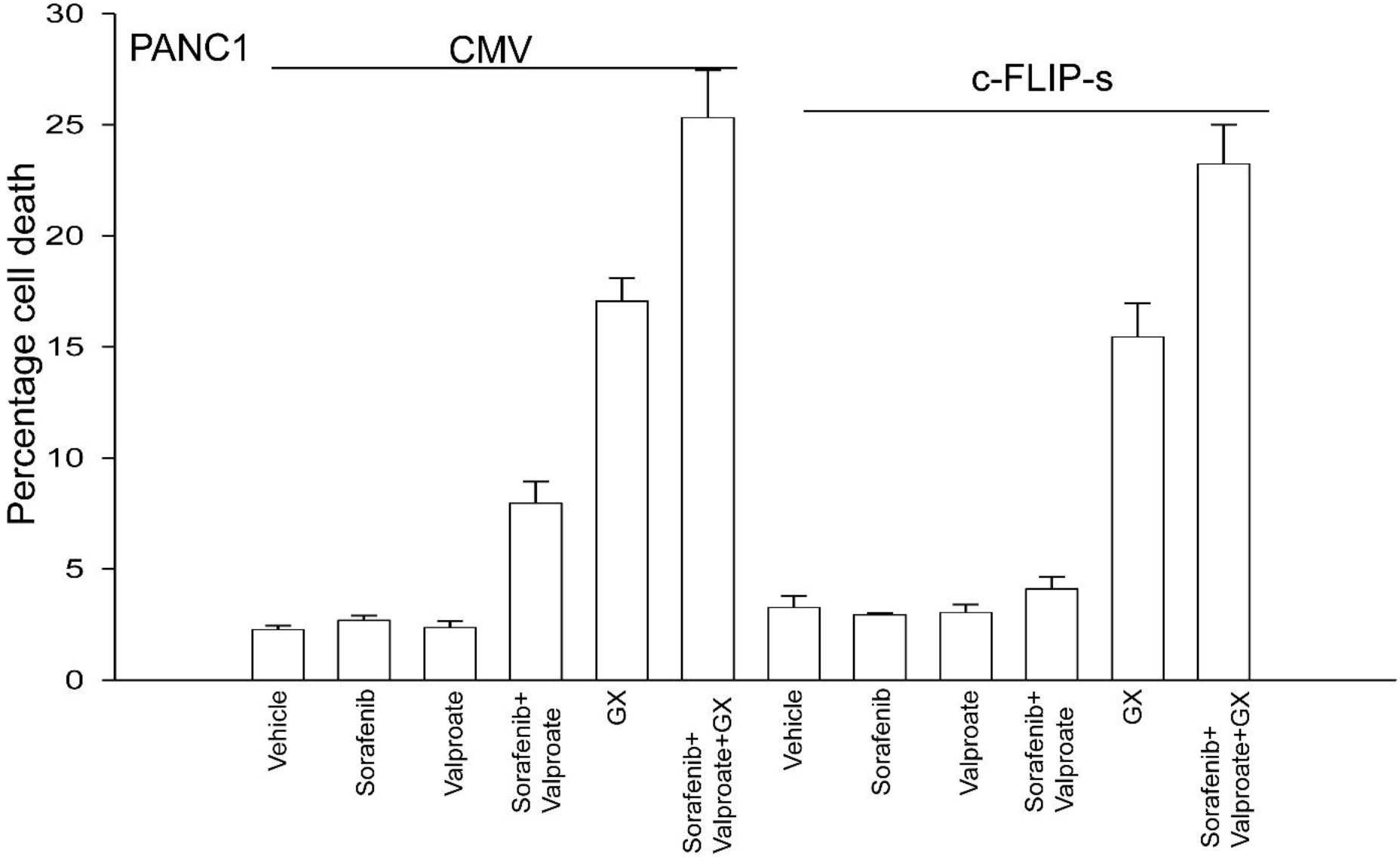
PANC1
CMV
c-FLIP-s
Percentage cell death
30
25
20
15
10
5
0
Vehicle
Sorafenib
Valproate
Sorafenib+ Valproate
GX
Sorafenib+ Valproate+GX
Vehicle
Sorafenib
Valproate
Sorafenib+ Valproate
GX
Sorafenib+ Valproate+GX

Figure 6B

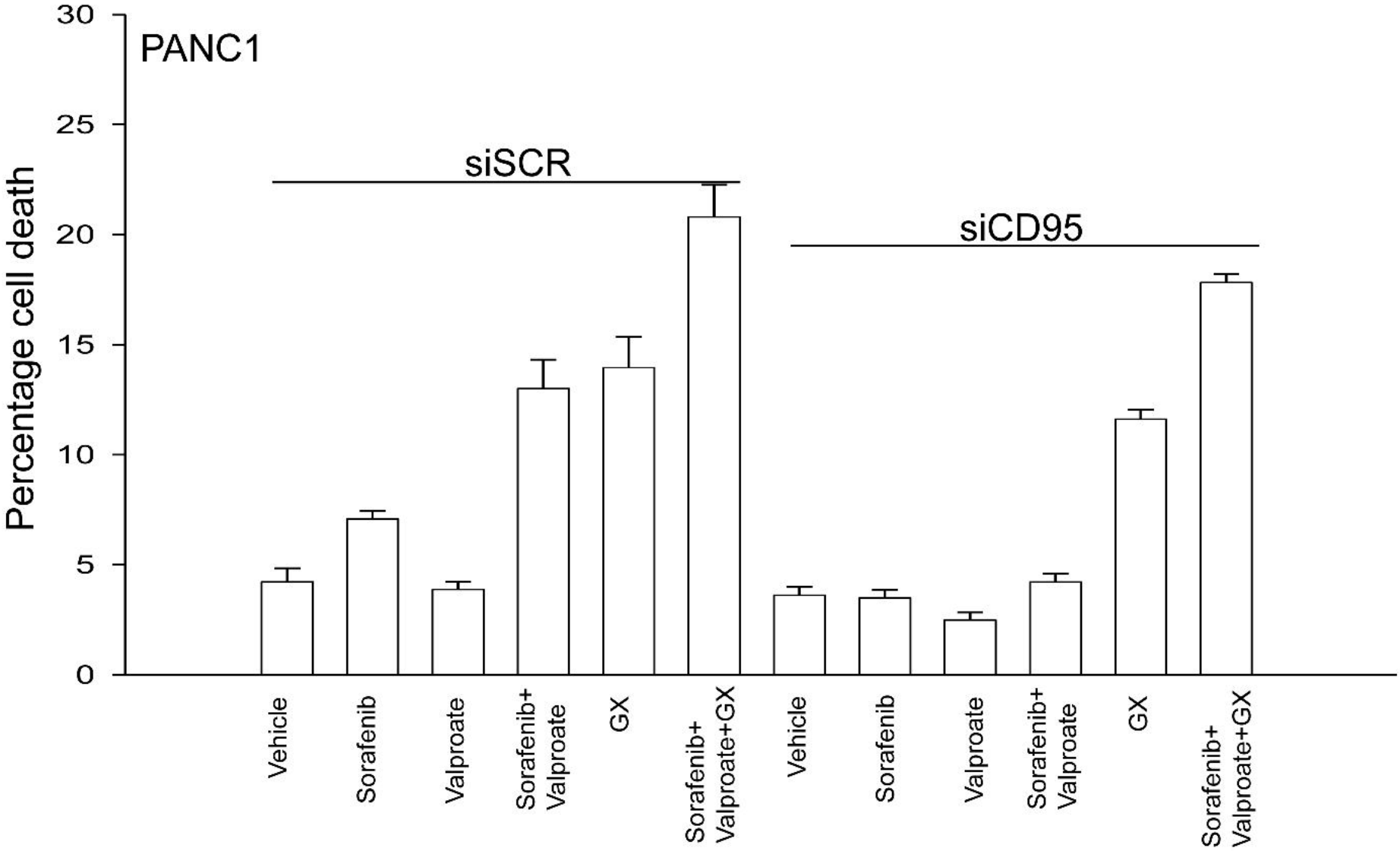
PANC1
Percentage cell death
30
25
20
15
10
5
0
siSCR
siCD95
Vehicle
Sorafenib
Valproate
Sorafenib+ Valproate
GX
Sorafenib+ Valproate+GX
Vehicle
Sorafenib
Valproate
Sorafenib+ Valproate
GX
Sorafenib+ Valproate+GX

Figure 6C

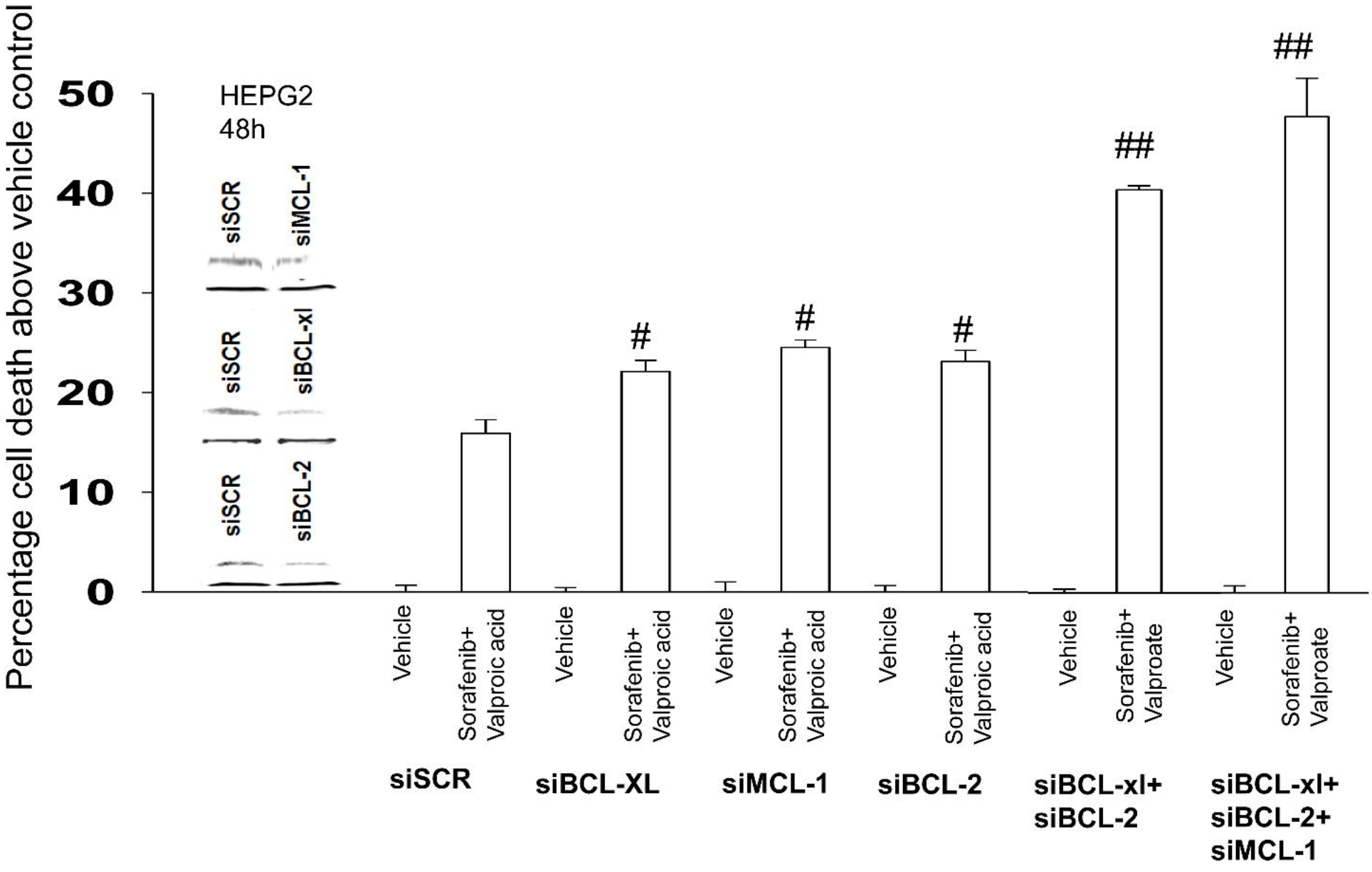
Percentage cell death above vehicle control
50
40
30
20
10
0
HEPG2
48h
siSCR
siMCL-1
siSCR
siBCL-xl
siSCR
siBCL-2
#
#
#
##
##
Vehicle
Sorafenib+ Valproic acid
Vehicle
Sorafenib+ Valproic acid
Vehicle
Sorafenib+ Valproic acid
Vehicle
Sorafenib+ Valproic acid
Vehicle
Sorafenib+ Valproate
Vehicle
Sorafenib+ Valproate
siSCR
siBCL-XL
siMCL-1
siBCL-2
siBCL-xl+ siBCL-2
siBCL-xl+ siBCL-2+ siMCL-1

Figure 6D

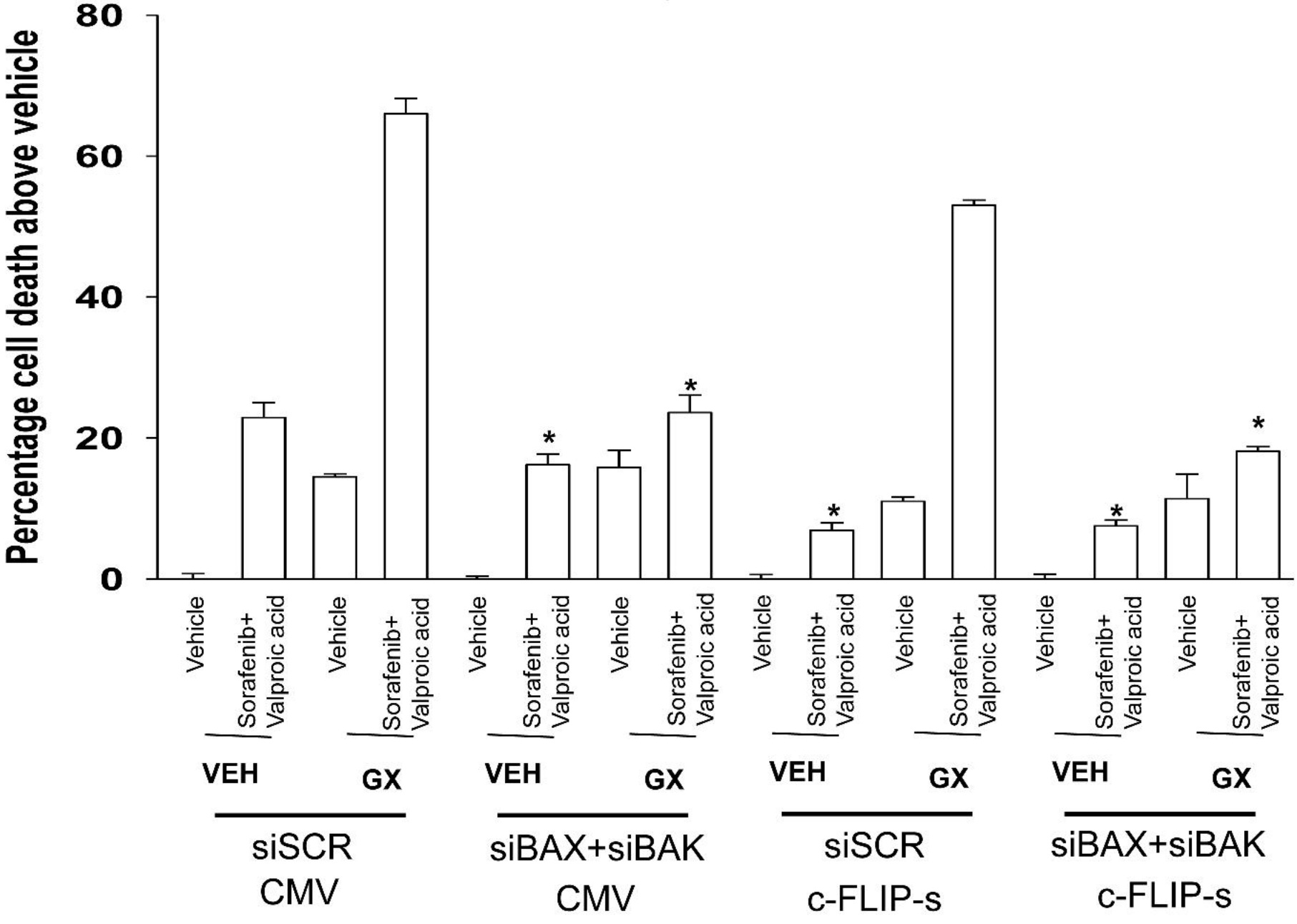
Percentage cell death above vehicle
80
60
40
20
0
Vehicle
Sorafenib+ Valproic acid
Vehicle
Sorafenib+ Valproic acid
Vehicle
Sorafenib+ Valproic acid
Vehicle
Sorafenib+ Valproic acid
Vehicle
Sorafenib+ Valproic acid
Vehicle
Sorafenib+ Valproic acid
Vehicle
Sorafenib+ Valproic acid
Vehicle
Sorafenib+ Valproic acid
*
*
*
*
*
VEH
GX
VEH
GX
VEH
GX
VEH
GX
siSCR CMV
siBAX+siBAK CMV
siSCR c-FLIP-s
siBAX+siBAK c-FLIP-s

Figure 7A

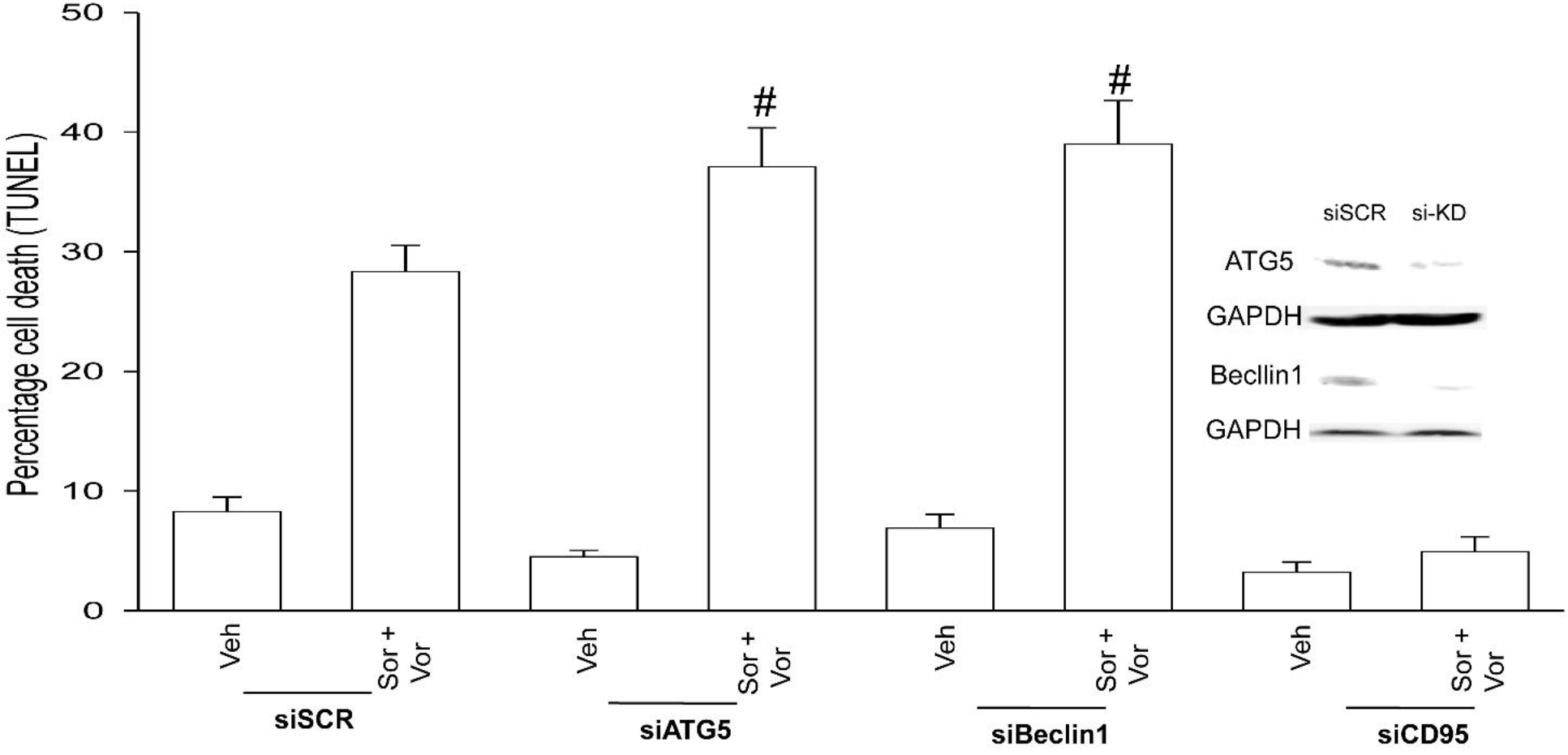
Percentage cell death (TUNEL)
50
40
30
20
10
0
#
#
siSCR
si-KD
ATG5
GAPDH
Becllin1
GAPDH
Veh
Sor + Vor
siSCR
siATG5
siBeclin1
siCD95

Figure 7B

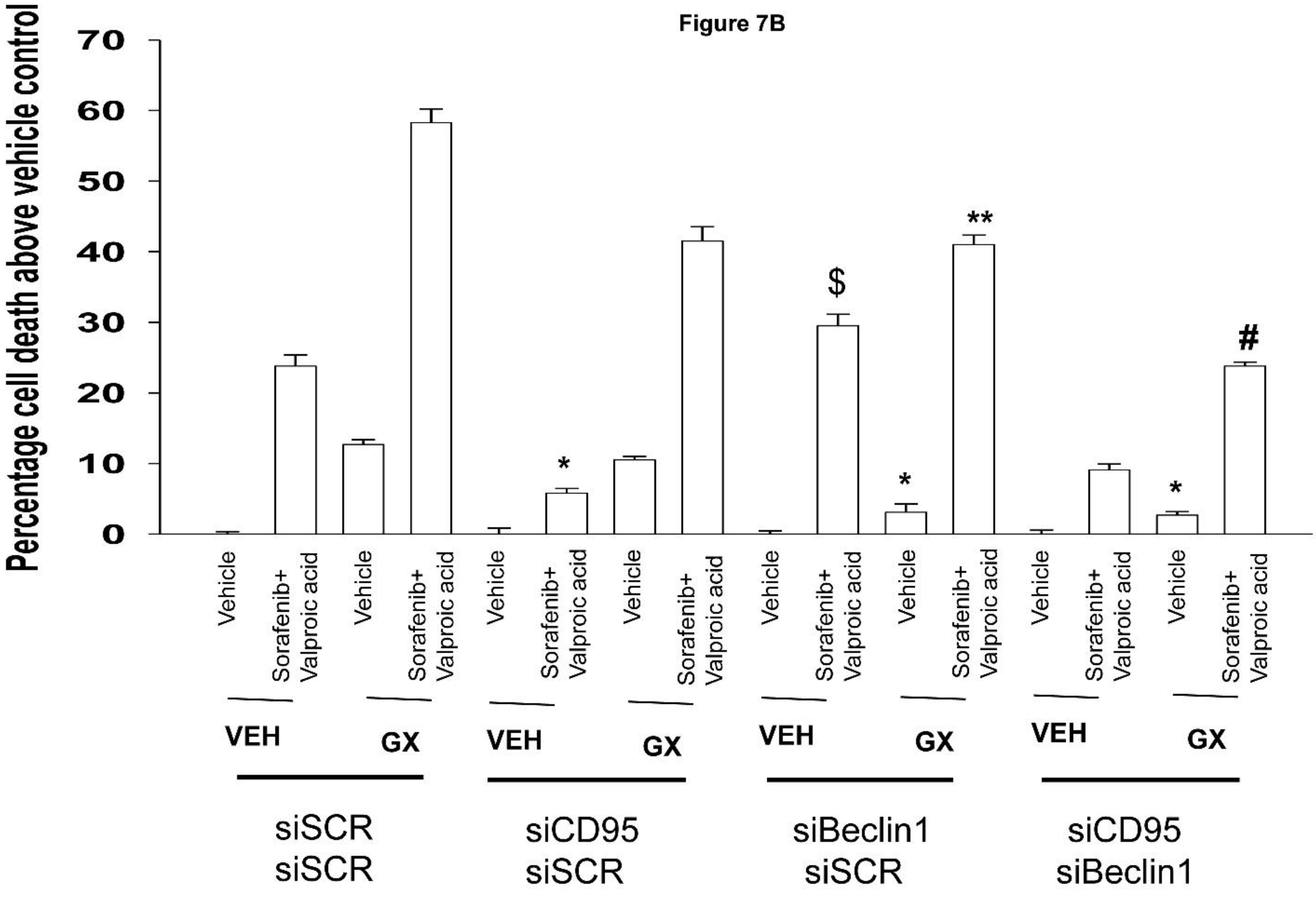
Percentage cell death above vehicle control
70
60
50
40
30
20
10
0
Vehicle
Sorafenib+ Valproic acid
Vehicle
Sorafenib+ Valproic acid
Vehicle
Sorafenib+ Valproic acid
Vehicle
Sorafenib+ Valproic acid
Vehicle
Sorafenib+ Valproic acid
Vehicle
Sorafenib+ Valproic acid
Vehicle
Sorafenib+ Valproic acid
Vehicle
Sorafenib+ Valproic acid
*
$
*
**
*
#
VEH
GX
VEH
GX
VEH
GX
VEH
GX
siSCR
siSCR
siCD95
siSCR
siBeclin1
siSCR
siCD95
siBeclin1

Figure 7C

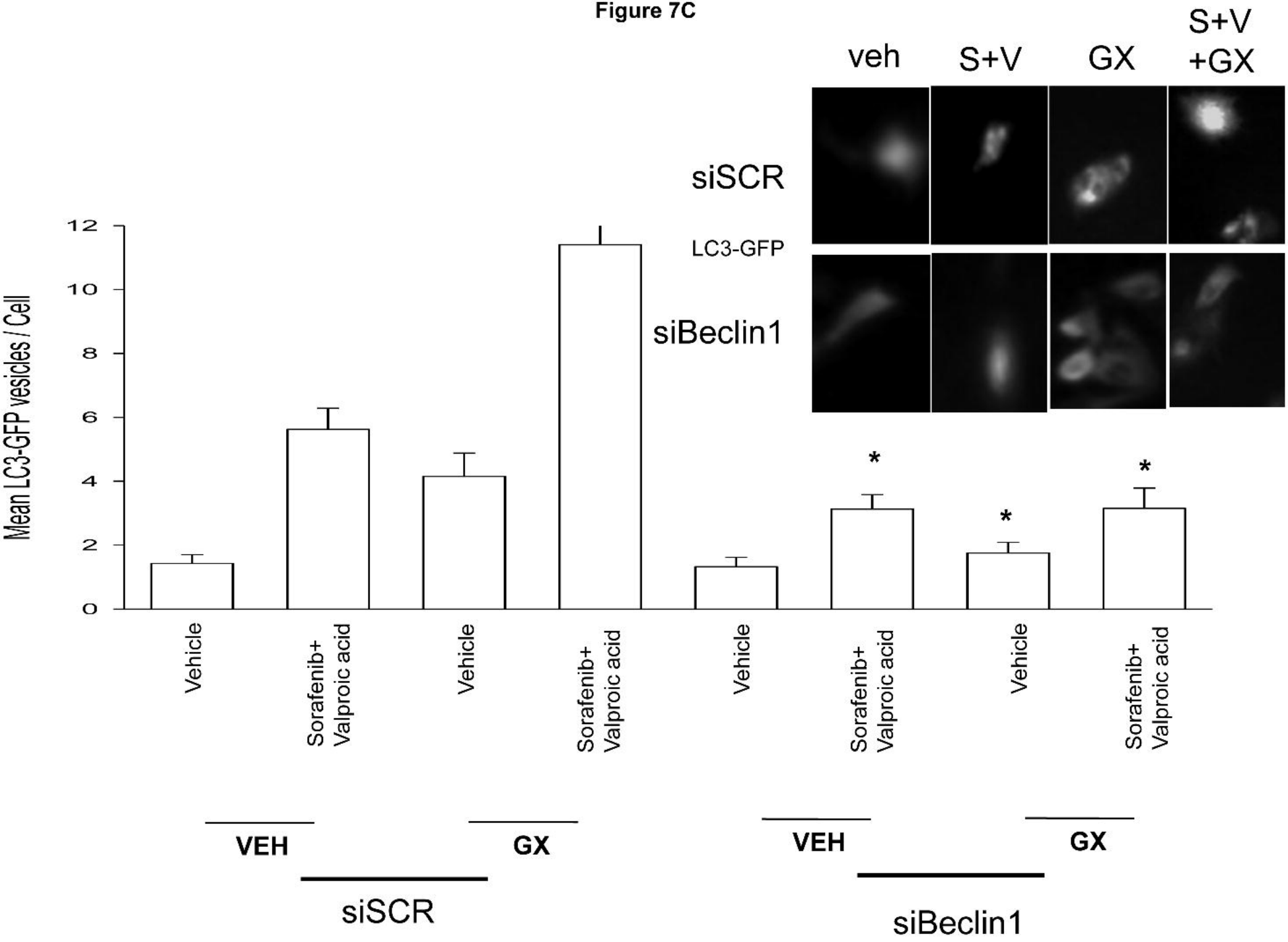
veh
S+V
GX
S+V
+GX
siSCR
LC3-GFP
siBeclin1
Mean LC3-GFP vesicles / Cell
0
2
4
6
8
10
12
*
*
*
Vehicle
Sorafenib+
Valproic acid
Vehicle
Sorafenib+
Valproic acid
Vehicle
Sorafenib+
Valproic acid
Vehicle
Sorafenib+
Valproic acid
VEH
GX
VEH
GX
siSCR
siBeclin1

Figure 7D

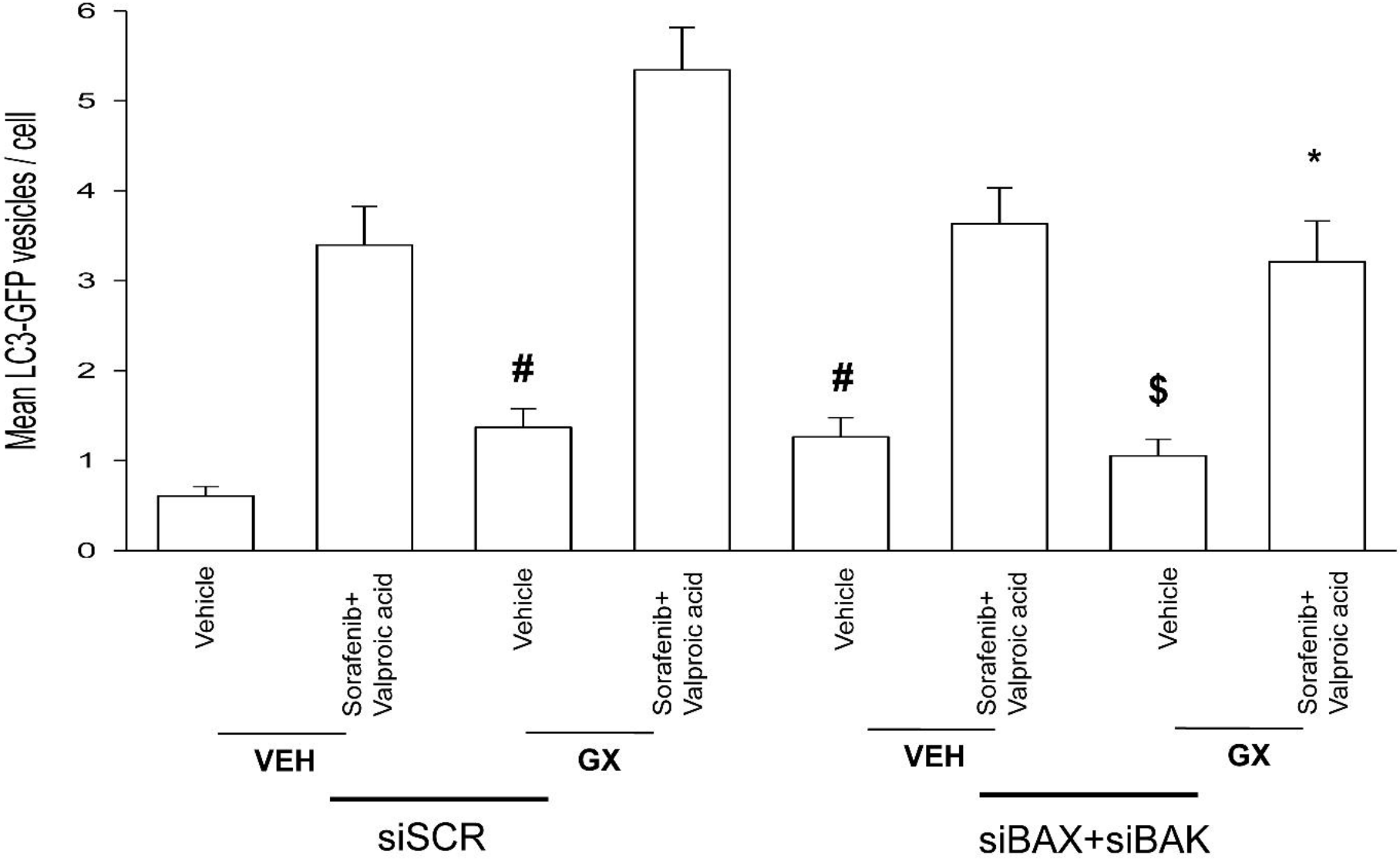
Mean LC3-GFP vesicles / cell
0
1
2
3
4
5
6
#
#
$
*
Vehicle
Sorafenib+ Valproic acid
Vehicle
Sorafenib+ Valproic acid
Vehicle
Sorafenib+ Valproic acid
Vehicle
Sorafenib+ Valproic acid
VEH
GX
VEH
GX
siSCR
siBAX+siBAK